OBSERVATION OF PULSARS AND OTHER SOURCES AT LOW RADIO FREQUENCIES

BY

FRANCISCO REYES

A THESIS PRESENTED TO THE GRADUATE COUNCIL
OF THE UNIVERSITY OF FLORIDA IN
PARTIAL FULFILLMENT OF THE REQUIREMENTS
FOR THE DEGREE OF MASTER OF SCIENCE

UNIVERSITY OF FLORIDA

1980

To Maria Angelica
Carolina
and Daniela

ACKNOWLEDGMENTS

I wish to express my deepest gratitude to my research advisor, Dr. Thomas D. Carr, for his guidance and encouragement, and his patience in reading and correcting the manuscript. It has been a privilege to work under him in this project, and I have benefited in many ways as his student.

I am also grateful to Dr. Alex G. Smith for providing me with financial support and for serving as a committee member. I give my appreciation to Dr. John P. Oliver for the development of the necessary hardware and software, for his advice and for serving as a committee member.

My deep appreciation goes to Dean Claudio Anguita and Professor Hugo Moreno of Facultad de Ciencias Fisicas y Matematicas of University of Chile for their encouragement and interest in my career and for providing me with financial support. I am also grateful to Jorge May and Juan Aparici for their encouragement and optimism and for providing me with the data at 45 MHz.

I wish to thank Jorge Levy for his help in the operation and calibration of the 26.3 MHz array, Chris St. Cyr for his encouragement and help in the computational part and Wesley Greenman and Richard Flagg for their help with the electronics.

My thanks goes to Hector Alvarez, Mauricio Bitrán and Fernando Oimos of Maipú Radio Observatory for their help with the 45 MHz data.

I am grateful to the Astronomy Department and the Physics Department and in particular to Drs. Heinrich Eichhorn, Robert J. Leacock, F. Eugene Dunnam, Charles F Hooper and Richard E. Garrett for their financial support in the form of teaching assistantships and fee waivers.

My gratitude goes to Mrs. Brenda Dobson for her patience in correcting my English and for her devotion in typing and editing the manuscript.

The realization of this project has been possible thanks to the continuous support provided to the radio astronomy program of the Department of Astronomy of the University of Florida and to the Maipú Radio Observatory through a grant from National Science Foundation (principal investigator Dr. Alex G. Smith).

TABLE OF CONTENTS

Abstract of Thesis Presented to the Graduate Council of the University of Florida in Partial Fulfillment of the Requirements for the Degree of Master of Science

OBSERVATION OF PULSARS AND OTHER SOURCES AT LOW RADIO FREQUENCIES

By

Francisco Reyes

December 1980

Chairman Thomas D Carr
Major Department Astronomy

The investigation of the radio emission spectra of pulsars at low frequencies is important since it helps to clarify the mechanism responsible for this emission. At the present, the low frequency end of the spectra is poorly determined compared with more precise measurements available at higher frequencies. Also, measurements of pulsar intensity variations at low frequencies due to scintillation are of value in the study of the interstellar medium.

Detection of pulsars at decametric wavelengths is difficult because of the deterioration of the signal-to-noise ratio caused by the high galactic background temperatures and the turn-over of the spectra of most pulsars. Also the dispersion of the pulses imposes the use of narrow bandwidth, reducing the sensitivity of the system.

Two pulsars have been observed at low radio frequencies using narrow bandwidth to avoid pulse dispersion problems. Pulsar PSR1133+16 was observed at 26.3 MHz using the University of Florida large array; pulsar PSR2045-16 was observed at 45 MHz using the Maipu Radioobservatory large array (Chile). Long term integration techniques were used to reduce the data.

Both pulsars were successfully detected and the average pulse intensity and integrated pulse profile were obtained. Time resolutions of P/38 were obtained for PSR1133+16 and P/62 for PSR2045-16, where P is the pulse repetition period. The two observed pulsars were selected because of their low dispersion measure, long period (>1 sec), high pulse intensity and their location with respect to the galactic background.

Several other radio sources were also observed and were used to calibrate the effective area of the 26.3 MHz antenna.

Thomas D Carr
Chairman

CHAPTER 1
INTRODUCTION

Pulsars were discovered in 1967 by S. Jocelyn Bell and Anthony Hewish. The first pulsar paper was published in Nature in February 1968 by Hewish et al. (1) telling about the discovery of pulsar PSR1915+21 and giving some of its parameters. Since then, about 321 pulsars have been detected and cataloged.

According to currently accepted models, pulsars are rapidly spinning neutron stars originating from supernova explosions. They are believed to have strong magnetic fields on the order of 10^{12} gauss, probably the strongest known magnetic fields in the Universe. The neutron star is believed to emit continuously a narrow beam of radio waves which corotates with the star, producing the observed pulse each time the beam sweeps past the earth. The periods of the pulses which have been observed range from about 0.03 to 4.3 seconds. So far, for only 2 pulsars has it been possible to find the optical counterpart of a pulsar.

Several mechanisms have been proposed to explain the origin of the radio emission and how the rotational energy of the neutron star is converted into electromagnetic wave pulses; this subject still remains one of the least understood aspects of pulsars. Some of the important parameters

of a pulsar that need to be measured before realistic models of the radio emission mechanism can be developed are the spectrum of the radiation, the pulse shape, peak intensity, and the time variations of these parameters. A large number of measurements have been made in the range of frequencies between 100 and 2,000 MHz, but only a few below 100 MHz (2). The low frequency part of the spectrum is particularly interesting because most pulsars present a turn-over of the spectrum at metric and decametric wavelengths, and also because pulse shape and widths show some peculiarities in this region. The spectral maximum for most pulsars is in the range 60 to 250 MHz; this peak is nearly symmetrical with respect to the frequency at which the maximum occurs (2). Measurements of the low frequency part of the pulsar spectra have been made by Bash et al at 38 MHz (3), Bruck and Ustimenko at 10, 16.7, 20 and 25 MHz (4, 5), Craft and Comella at 40 MHz (6) and more recently by Izvekova et al at 61 and 102.5 MHz (7, 8).

Most pulsars measured at low frequencies are in that part of the sky which is observable from northern hemisphere observatories. Observations at the lowest frequencies have been carried out in the southern hemisphere only by Australian observatories, at 80 and 150 MHz (9, 10). Detection of pulsars at low radio frequencies is difficult because of the deterioration of the signal-to-noise ratio caused by the high galactic background temperatures, and the low frequency spectral turn-over exhibited by most

pulsars. The pulse dispersion in the interstellar medium becomes more severe the lower the frequency. At higher frequencies, compensation can be made for dispersion, permitting the use of relatively high bandwidths. However, at the lower frequencies, it is generally necessary to restrict the bandwidth because of dispersion, further reducing the sensitivity of the detection system. Due to the intrinsic short pulse durations of most pulsars ($\leq$ 150 msec), short time constants must be used, imposing still another limitation on the sensitivity of the system.

Nevertheless, the sensitivity of the system can be improved by averaging many independent records of the same source. If N records are averaged, the signal-to-noise ratio (S/N) is improved by a factor of $\sqrt{N}$. For pulsars, this can be accomplished by averaging groups of consecutive periods. Digital sampling is generally used in such averaging. Due to the relatively short pulsar periods, the signal needs to be sampled at a fast rate in order to have enough time resolution to meet the requirements of the sampling theorem. Since it is not feasible to manipulate the large amounts of data generated in the digitizing process by hand, digital computing techniques must be used, providing an efficient way to average, process, store and plot that data.

In the past few years, the development of small and inexpensive microprocessors has made possible improved methods of pulsar data handling and processing. If the

period of a pulsar is known to be a good accuracy, it is possible to average many periods (N typically in the range of a thousand periods), greatly improving the S/N ratio.

The University of Florida Radio Observatory, located in Dixie County about 50 miles west of Gainesville, and the Maipú Radioastronomical Observatory of the University of Chile, located 20 miles southwest of Santiago, have long been engaged in a cooperative program of low frequency radio astronomy. Although most of the effort over the years has gone into the study of Jupiter's radio emission, other decameter-wavelength sources are also investigated. Each of the two observatories has a very large antenna array, in addition to many smaller radio telescope antennas. The Florida array consists of 640 dipoles operating at a center frequency of 26.3 MHz, while the Chile array has 528 dipoles and operates at a center frequency of 45 MHz. Both arrays were believed to be suitable for observing pulsars, although previous attempts to use them for this purpose had not been successful.

The goal of the research on which this thesis is based was to develop a low frequency pulsar data acquisition and reduction system, and to use it to detect and measure the important parameters of at least one pulsar with each of the two large arrays (i.e. the one in Florida and the one in Chile). This goal was achieved.

CHAPTER 2
DATA ACQUISITION AND REDUCTION

Two pulsars, PSR1133+16 and PSR2045-16, were selected (from the lists in Appendix A) for observation because of their low dispersion measure, relative long period (>1 second), high pulse intensity and favorable location with respect to the galactic background. Pulsar PSR1133+16 was observed at 26.3 MHz using a bandwidth of 8 kHz, and pulsar PSR2045-16 was observed at 45 MHz with a bandwidth of 10 kHz.

The detected IF signals of the pulsar were recorded on one channel of a magnetic tape, and a time code generator signal on the other channel. The tapes were played back (making a 4:1 slow down), the pulsar signal sampled, and the resulting values stored in the NERDC Amdahl 470 computer. The time code generator signal provides the timing pulses for the sampling and also indicates Universal Time (U.T.). The sampling of the signal was accomplished by a 12 bit analog/digital converter (A/D) and a KIM I microprocessor. Pulsar pulse averaging is carried out by a computer program which averages consecutive periods of the sampled pulsar signal, previously stored in the Amdahl computer.

2.1 Data Acquisition of Pulsar PSR1133+16

The pulsar PSR1133+16 was observed for 20 nights between April 25, 1979, and June 8, 1979, using the University of Florida 26.3 MHz large array, located at the University of Florida Radio Observatory in Dixie County. The 26.3 MHz array is a nearly filled rectangular array of 640 half-wave dipoles that covers about 30,000 m^2. The half power beamwidth (HPBW) is 2.5° north-to-south by 6.0° east-to-west. It is a phase steered array with full N-S directional control of the beam in quarter-beamwidth increments, and a selection of 8 E-W beam directions spaced one beamwidth apart. Phasing is accomplished by means of a network of Butler matrices, hybrid rings and plug-in phasing cables.

North-south phasing of the array for a source having a given declination is accomplished in two ways, a coarse adjustment in large increments of declination and a fine adjustment providing small steps. A change in the coarse phasing requires the replacement of many plug-in cables located throughout the array, and requires about 2 or 3 man-hours of labor. Fine phasing for the desired declination is quickly accomplished by means of switches at a single location. The beam pointing can be altered in small increments to any declination within a strip roughly 10° wide by means of the fine phasing controls. Positioning the beam to a new declination outside this strip requires a coarse phasing readjustment. The right ascension of the beam is of course

controlled by the rotation of the earth. Scans in, in all of the 8 selectable east-west beams (designated 4E, 3E, 2E, 1E, 1W, 2W, 3W, 4W) are made by starting each scan at the appropriate sideral time. A computer program called ARRAY developed by Dr. M. D. Desch, is used to obtain information on cable lengths required for coarse phasing, switch positions for fine phasing, and beam transit time across the desired source (11). A more detailed description of the antenna and its adjustment has been given by Desch, (12) and Daesch et al. (13).

In order to use the maximum gain of the array, only the central E-W beam positions 2E, 1E, 1W and 2W were used, and within each beam only the central portion of it was recorded (~8 minutes each beam). A maximum of 32 minutes was recorded each night. Pulsar PSR1133+16 was selected because of its relatively high pulse energy ($\sim 0.75 \times 10^{-26}$ $Wm^{-2}Hz^{-1}$ at 61 MHz), long period (1.188 s), and low dispersion (DM ~ 5 parsec cm^{-3}). It was also easy to reach this pulsar using the phasing the antenna had at that time (phased to make Jupiter observations), without having to completely rephase the array. Only the fine phasing needed readjustment. During the period in which the pulsar was observed, it was transiting at about midnight.

Only 8 nights (out of the 20 observed) gave reliable data, free from static and stations. The end of the observation period coincided with the beginning of the thunderstorm

[redacted] at which time [redacted] down for the summer.

A block diagram for the interconnections of the equipment used to observe the pulsar is shown in Figure 2.1. The equipment basically included a Collins R 390 receiver, a Magnecord 1022 magnetic tape recorder, a Tracor 5D frequency standard, and a Systron Donner 8154 time code generator/reader.

The time code generator (TCG) was synchronized against WWV; this was accomplished by triggering an oscilloscope with the 1 pulse per second (1 PPS) output of the TCG and measuring the delay of WWV 1 PPS. The 1 PPS of the TCG was brought as close as possible to the 1 PPS of WWV (usually between 5 to 20 ms) by making short interruptions of the 1 MHz signal from the Tracor frequency standard. The delay between the two 1-PPS pulse trains was measured to an accuracy of about ±0.5 ms, and from that information the U.T. was obtained, except for the propagation delay between Boulder, Colorado, and Dixie County Radio Observatory. No corrections have been made for this delay because no attempt was made to relate the epoch of this observation with any other observations.

The measured drift of the Tracor time standard is about 80 μs/h; this causes a drift in the epoch of about 100 μs between pulsar transits by beams 2E and 2W ($\sim 1^h 16^m$), this drift is small enough to be noticed, considering the time

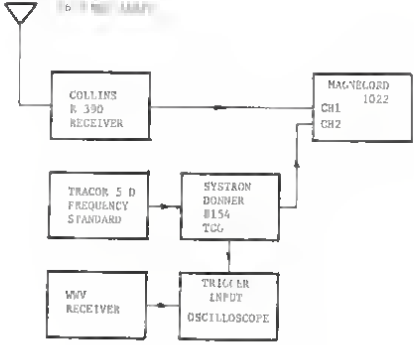

Figure 2-1 Block diagram of the equipment interconnections used to record pulsar PSR1133+16

resolution of [illegible] ms (P/38, P = period obtained for this pulsar.

The detected IF output of the receiver was recorded on channel 1 of the Magnecord at 15 IPS and the recording level for the galactic background was set to about 7 VU on the recording level monitor, to prevent any saturation during signal peaks.

The time code generator was recorded on channel 2 of the Magnecord. This signal serves a double purpose: it provides a time reference for the pulsar signal, and later on, in the data reduction process, provides the timing signal for the KIM I microprocessor.

As a back-up to obtain the correct time, at the beginning of each observing session the WWV signals were recorded on channel 1 (the TCG also on channel 2) for about 2 5 minutes. The correct time can be obtained by measuring the delay between the 1 PPS of WWV and the 1 PPS of the TCG.

The receiver was tuned to a center frequency of 26.3 MHz and the bandwidth set to 8 kHz. Using data for higher frequencies an extrapolated pulse width (at the base) of about 80 ms was obtained. Pulse broadening due to dispersion (DM = 5 parsec cm^{-3}) is about 18 ms (for a bandwidth $\Delta\nu$ = 8 kHz), which was considered acceptable.

2.2 Data Acquisition of Pulsar PSR2045-16

Pulsar PSR2045-16 was observed for 11 nights between May 15 and May 30, 1979, using the Maipú Radio Astronomical

Observatory 45 MHz large array, located about 20 km south-west of Santiago, Chile. The 45 MHz array is a filled rectangular array of 528 full-wave dipoles with an effective area of 12,000 m^2. It is a transit instrument with 6 independently phased subsections in the N-S direction and can be oriented to a zenith angle of about ±45° in the meridian plane. The HPBW is 2.1° north-to-south by 4.6° east-to-west. A multiple beam system is generated by a Butler matrix. A more detailed description of the array has been given by Reyes (14) and May et al. (15).

Pulsar PSR2045-16 was recorded for 20 minutes each night, which is the time it takes to drift between the E-W 3 dB points of the beam. This pulsar was selected because of its relatively high pulse intensity ($\sim 1.0 \times 10^{-26} Wm^{-2} Hz^{-1}$ at 34 MHz), long period (1.96 ms) and its low dispersion measure (DM = 12 parsec cm^{-3}). A zenith angle of only 18° at transit was also another favorable factor considered.

The equipment used for the data acquisition of this pulsar consisted of a modified General Dynamics telemetry receiver, a Magnecord 1022 magnetic tape recorder, a Systron Donner 8220 TCG and a Rhode and Schwartz quartz time standard. The interconnections are similar to those shown in Figure 2-1. During the observing sessions the pulsar was transiting at dawn, and no interference was noticed. Nine of the eleven nights gave reliable data; the other two nights were discarded because of equipment malfunctions.

A bandwidth of 10 kHz was used, this is the minimum bandwidth of the receiver. Using data obtained at higher frequencies, an extrapolated pulsar pulse width at the base of about 130 ms was obtained at 45 MHz. The pulse broadening due to the 10 kHz bandwidth is 11 ms. This was considered soceptable.

The quartz time standard is checked daily against the Chilean National Observatory cesium time standard; the epoch is believed to be known with an accuracy of about ±10 μs. The drift in time is about 3.6 μs/h (or about 0.00190 μs/P, where P = 1.96 s, the pulsar period). The drift is 1.2 μs in the 20 minutes between the east-to-west HPBW. For all practical purposes considered in this research, this is negligible.

2.3 Data Reduction

Data reduction for both pulsars was performed using the facilities of the Department of Astronomy of the University of Florida in Gainesville. The basic configuration and interconnections of the equipment for data reduction are shown in Figure 2-2. The schematics for the most relevant blocks are presented in Appendix C.

As stated earlier, the IF signal in the receiver is band limited to 8 or 10 kHz and appropriately smoothed. The resulting audio frequency signal is recorded in analog form on channel 1 of the Magnecord tape recorder at a tape speed of 15 IPS. The time code generator is recorded on channel 2.

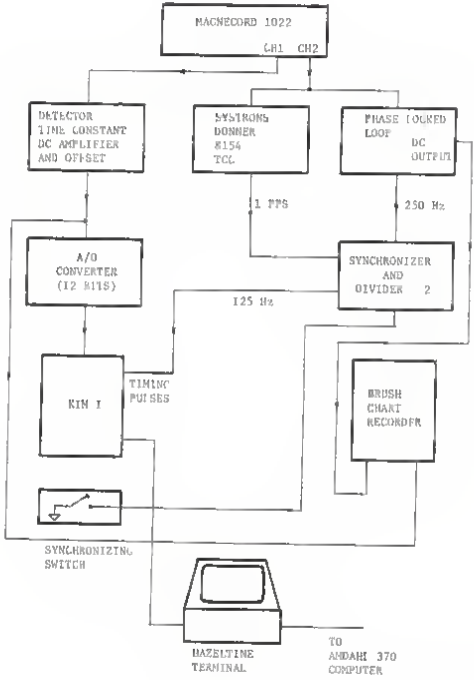

Figure 2-2 Block diagram of the data reduction equipment

In order to achieve the desired time resolution and to be able to sample the data at an appropriate rate, the magnetic tapes were played back at 3 3/4 IPS, providing a slow down of 4 to 1.

Pulsar signals from channel 1 of the Magnecord are sent through a diode detector and smoothing filter to the 12 bits A/D converter. The filter time constant was adjusted to 45 ms for both the rising and falling edges of the noise pulses.

The TCG signal from channel 2 of the Magnecord is connected to the input of the TCG (working now as a reader) to provide both a visual display of the time and a 1 PPS pulse (taken from a modified output). The latter gives the synchronizing signal to start the sampling of the data at a precisely known time. It is particularly important to know the time at which the sampling is started in order to be able to combine in phase 2 or more blocks of data.

In order to obtain the timing signal for the KIM I, the TCG signal from channel 2 of the Magnecord is connected also to a phase locked loop (PLL) circuit. The PLL circuit locks at a particular frequency of the signal, filtering out the rest of the frequencies present in the complex wave form of the TCG signal. The 1000 Hz signal of the TCG is transformed to 250 Hz due to the 4 to 1 slow down. The PLL was carefully tuned to 250 Hz, and the output then divided by 2. The resultant 125 Hz constitutes the timing signal for the KIM I.

A gated DC output from the PLL circuit was monitored on a Brush Mark II chart recorder. This provides a good means

to detect any [illegible] synchronism or dropout of the T[illegible] playback signal. If there is any loss of synchronism between the input and PLL signals, then the gated DC output falls to zero, giving a visual indication to stop the sampling process. If synchronization were lost, the pulsar signals would be averaged out of phase, wiping out any pulse at the end of the integration process. A means was provided for starting the sampling at the next 1 PPS pulse from the TCG occurring after a switch was thrown. This made it possible to know the exact time at which sampling started. This was accomplished by connecting the start switch to the D input and the 1-PPS signal to the clock (C) input of a D-type flip-flop. The output of the flip flop gates the 125 Hz signal in a NAND gate (see schematic in Appendix C). When the start switch is turned on, the next 1 PPS of the TCG enables the 125 Hz signal to go into the KIM I and the sampling is started.

The sampled values (coded in hexadecimal) are sent through the Hazeltine terminal to the Amdahl 470 computer and stored there for further processing and analysis.

Since the maximum number of cards that can be stored under a new data file name is 493, it was necessary to break up the data into several "blocks" to meet this requirement. The 8 minutes of data obtained in one beam for pulsar PSR1133+16 were broken up in 2 blocks of 4 minutes each, generating about 312 cards for each block (for a TSAMP= 02 and timing signal frequency = 125 Hz, see Appendix B). The

20 minutes of data obtained each night for pulsar PSR2045-16 was broken up into 4 blocks of 5 minutes each, generating about 390 cards for each block.

The method of breaking up the data into blocks proved to be useful also because one can inspect the results of the average of each block separately, making it possible to search by eye for a possible pulse that might appear at the same location in the different blocks. It is highly unlikely that interference transients would appear in the same location in each of several blocks.

Monitoring of the DC gated output of the PLL circuit is very useful since synchronism is sometimes lost when a tape is played back. If that happens, then that portion of the tape is skipped and a new block started.

The KIM I program which is necessary to digitize the data is loaded into the microprocessor from a cassette tape recorder.

2.4 Block Designation for Each Pulsar

Many blocks of data were generated in the data reduction process. In order to avoid any confusion with the data and to be able to distinguish quickly between blocks, a designation scheme was developed for referring to a specific data block. The designation format contains in abbreviated form the pertinent information for that block. For pulsar PSR1133+16, the following block designation was adopted:

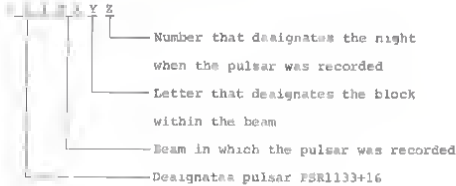

The beam designations are as follows:

2E 2nd beam east of transit

1E 1st beam east of transit

1W 1st beam west of transit

2W 2nd beam west of transit

In order to distinguish between the different blocks within a given beam, a capital letter was used, usually A and B. In case it became necessary to break up the data into more than two blocks (i.e. due to loss of synchronism of the TCG signal) C was also used.

The indicator for the data of the night on which the pulsar was observed was an integer, as follows:

Night	Date
1	April 25, 1979
2	April 27, 1979
3	April 28, 1979
4	April 30, 1979
5	May 20, 1979
6	May 25, 1979
7	May 26, 1979
8	May 30, 1979

The designation scheme for the blocks of data from pulsar PSR2045-16 is slightly different, as follows:

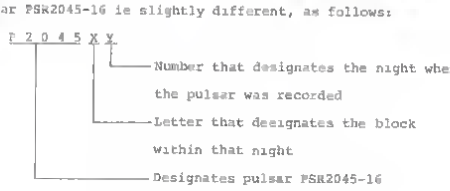

The block designation is usually one of the letters A, B, C, D, E or F.

The nights were numbered as follows.

Night	Date
-1	May 15, 1979
1	May 16, 1979
2	May 17, 1979
3	May 18, 1979
4	May 19, 1979
5	May 22, 1979
6	May 23, 1979
7	May 24, 1979
8	May 29, 1979
9	May 30, 1979

The reduced data for each block was stored on a disk called UF.B0030601.S5-XXXXX, where XXXXX is the name of the block. The data have been recorded also on a digital magnetic tape called PULSAR.

4.5 Computer Programs for Data Reduction

In order to analyze the data and to plot the values, a set of two computer programs called PULSAR and MCAFGM are used. The basic parameters necessary to analyze the data must be given to the PULSAR program, they are:

N = Number of bits digitized (=12)

TPP = Timing pulse period (ms)

NPA = Number of pulse intervals averaged

P = Pulsar period (s)

PLOFF = Plot offset

MAG = Plot magnification factor

The MCAFGM program (using the PULSAR program parameters) takes the first group of pulse intervals to be averaged (NPA) from the data of a particular block and calculates the overall average and the standard deviation. These two quantities, and the average for each bin, are plotted. The program next takes the second set of intervals from the data and does the same as before. Also the first set of intervals is averaged with the second set, computing a new average (cumulative) for each bin, an overall average, and a new standard deviation and plots the values for the bins. This process continues including each time the next group of intervals (NPA).

The first set of programs is run once only to check the quality of the data, to detect any problem and to obtain the total overall average for a block which will be used in a second run.

The second set of programs called PULSITO and MCAFGM1 is similar to the already described PULSAR and MCAFGM, but

this time, the data is taken from disk (where it has been previously stored), produces a magnified plot and punches cards with the final values for each bin, the total block average and the final standard deviation. This set of cards is used later on, to stack 2 or more blocks.

Usually after the process already described, the digitized data is recorded on the PULSAR magnetic tape and released from the data files.

In order to stack 2 or more blocks, the sets of cards of each block (except the first, which is used as reference) is shifted the proper number of bins so that the bins can be averaged in phase. The number of bins to be shifted in each block is given by the following relationship:

$$N_{bins} = \frac{\left\{-\left[\text{Frac}\left(\frac{T_i - T_1}{P}\right)\right]+1\right\}\times P}{R} \qquad (2\text{-}1)$$

where N_{bins} = Number of bins the block i needs to be shifted with respect to block 1

T_1 = Time start sampling block 1

T_i = Time start sampling block i

P = Pulsar period

R = Time resolution $\left(= \frac{P}{\text{Number bins}}\right)$

Frac = Fractional part

The fractional part of $\frac{T_i - T_1}{2}$ corresponds to the fraction of the period between the time of beginning of block i and the time of beginning of the first block. The relationship given by 2-1 was evaluated using an HP-29C calculator.

A last program called P2045 (or P1133) reads the cards of the blocks to be averaged (previously shifted), calculates the average for each bin (weighting by the number of periods in each bin), computes the final average of the combined blocks, the standard deviation σ, and plots the data. Also plotted is the 3σ reference line, which is used as a reference to aid in deciding whether or not a pulse was present at the end of the averaging.

The KIM I program to digitize the data and the MCAFGM program were developed by Dr. John F. Oliver; MCAFGM1 is a modification, made to adapt it to the use previously explained.

A program called DOPVEL was used to obtain the apparent pulsar period for the night and time when the pulsar was observed. This program gives the pulsar period at a particular site and at a given time, correcting for Doppler shift due to the earth's rotational velocity and its motion around the sun. This program was developed at the NRAO by Drs. R. N. Manchester and R. A. Gordon and made available by Dr. Steve T. Gottesman.

Finally a summary of the times spent observing and reducing pulsar data and the total time of terminal use is presented in Table 2-1.

Table 2-1 Summary of time spent with pulsar data.

Pulsar	Total Time Observing Pulsar	Total Time of Data Reduced	Total Time Digitizing Data
PSR1133+16	$10^h\ 40^m$	$4^h\ 10^m$	$16^h\ 04^m$
PSR2045-16	$3^h\ 40^m$	3^h	12^h

CHAPTER 3
DATA ANALYSIS

3.1 PSR1133+16 Data Analysis

From the 8 nights of data reduced for pulsar PSR1133+16 (26.3 MHz, Florida), pulses were found with no ambiguity on 2 nights. Pulses were found on April 28 and May 25, 1979, over averages of 340 and 390 periods respectively; the results are plotted in figures 3-1 through 3-7.

On April 28, after averaging over 340 periods ($\sim 6^m 44^s$) a pulse appears in bin 33 with an amplitude of $\sim 3\ \sigma$ above the mean value (Figure 3-1). The 2 data blocks P112EA3 and P112EB3 used to obtain this final block have been plotted separately in figures 3-2 and 3-3. It can be seen that a pulse appears in both blocks at the same location (bin 33). Even though the pulse appearing in each block would not alone be considered to be statistically significant, the fact that they appear in the same location for two separated sets of data provides an excellent test of the validity of the pulse.

On May 25, after averaging over 390 periods, a prominent pulse was obtained in bin 25 with an amplitude of 3.4 σ, this pulse is shown in figure 3-4. The same test for validity as before was made. Blocks P112WA6 and P112WB6 are

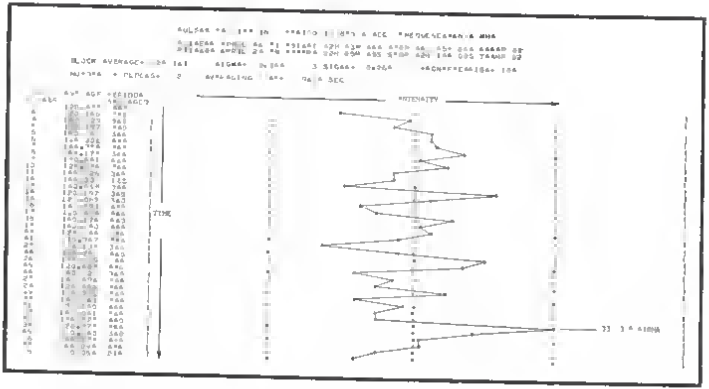

Figure 3-1 Pulsar PSR1133+16 (Blocks P112EA3 and P112EB3) recorded at 26 3 MHz on April 28, 1979 Average over 340 periods.

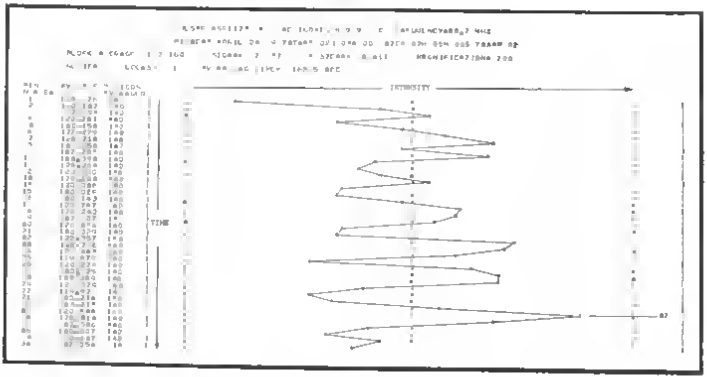

Figure 3-2 Pulsar PSR1133+16 (Block P112EA3) recorded at 26.3 MHz on April 28, 1979. Average over 140 periods.

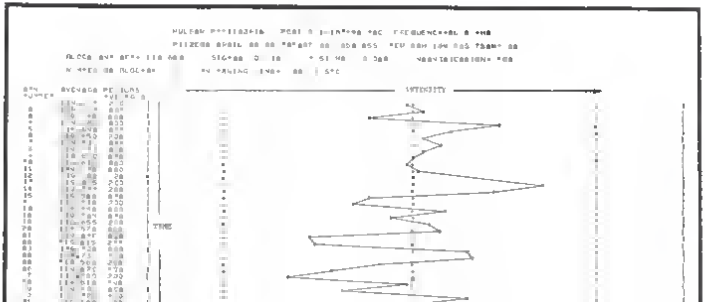

Figure 3-3. Pulsar PSR1133+16 (Block F112EB3) recorded at 26.3MHz on April 28, 1979. Average over 200 periods

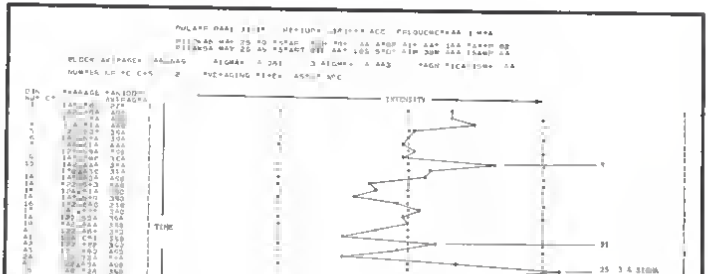

Figure 3-4. Pulsar PSR1133+16 (Blocks P112WA6 and P112WB6) recorded at 26.3 MHz on May 25, 1979. Average over 390 periods.

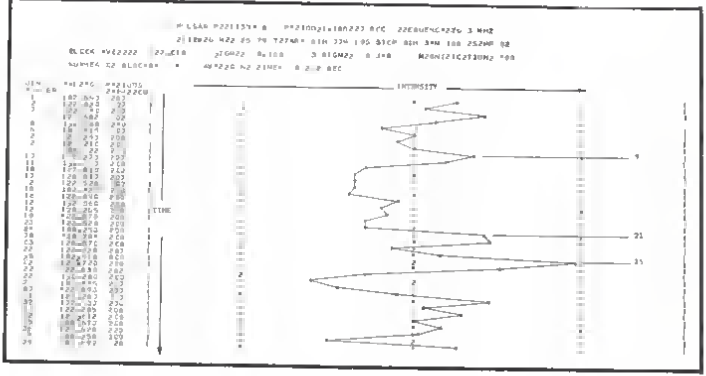

Figure 3-5 Pulsar PSR1133+16 (Block P112WA6) recorded at 26.3 MHz on May 25, 1979. Average over 200 periods.

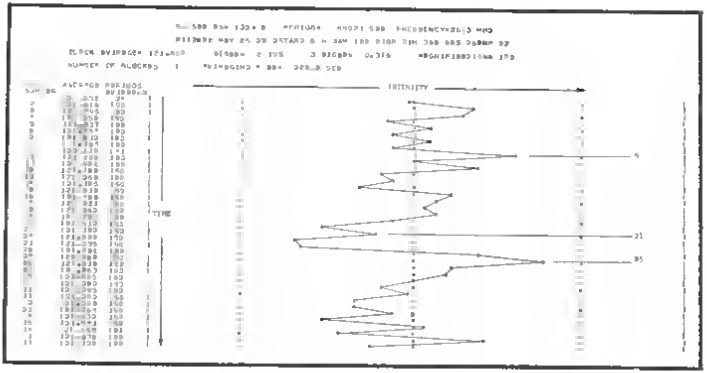

Figure 3-6. Pulsar PSR1133+16 (Block P112NB6) recorded at 26.3 MHz on May 25, 1979. Average over 190 periods.

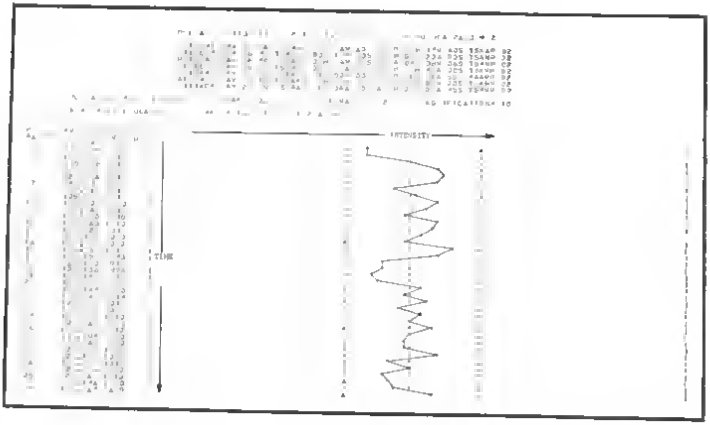

Figure 3-7. Pulsar PSR1133+16 recorded at 26 3 MHz on May 26, 1979 No pulse present

plotted separately in figure 3-5 and 3-6 A pulse appears in bin 25 in block F112WA6, with an intensity 2.6 σ above the mean value, also in block F112WB6, the pulse is weaker, being only 2.3 σ, but is at the same location (bin 25) Once again we have the fact that 2 pulses appear in the same location in two independent sets of data.

From a precise knowledge of the pulsar period and the elapsed time between the April 28 and May 25 appearances of the pulse, it should be possible to preserve its phase so that it would reappear in the same bin on the second date as it occupied on the first. However, this could not be done because of the period uncertainty. This problem will be addressed later when analyzing PSR2045-16 data.

The pulsar was detected in only one beam on each of the two nights, disappearing when the beam was switched to the next position. This phenomenon will be discussed later in the conclusions, when polarization effects are considered.

Before other tests made on this pulse are discussed, it is interesting to note that in bins 9 and 21 of block F112WA6 (figure 3-5) two more small pulses can be distinguished. Although neither of them alone would be considered statistically significant, they both seem to appear again in block F112WB6 (figure 3-6) in the same position. The pulse in bin 21 leads the main pulse in bin 25 by 125 msec (resolution ~31 msec/bin) or approximately 38° of phase

The pulse in bin 9 is separated by 496 msec from the main pulse, which is about 150° (or 0.42 P, P = 1.88023 sec)

The pulse in bin 21 suggests the existence of a subpulse leading the main pulse. Several authors have indeed reported for this pulsar a complex main pulse composed of 2 subpulses, the leading subpulse decreasing in intensity with respect to the trailing subpulse as the frequency decreases (6, 7, 8). The separation between the two subpulses has been measured at higher frequencies and extrapolation from that data suggests a much closer separation for low frequencies than the separation obtained at 26.3 MHz between the pulses in bins 21 and 25. In 1972 Bruck and Vatimenko (4) reported some observations made at 25 MHz with a linearly polarized antenna; they found that this pulsar shows a variety of pulse shapes with rapid transitions from one to another. In one plot, they show a pulse composed of 2 subpulses and separated by ~148 msec. Despite the poor resolution used (P/16 or ~74 msec), the 2 subpulses are clearly defined.

The separation of the subpulses as a function of frequency has been plotted in figure 3-8, including the result by Bruck and Vatimenko and our result (i.e. for the bin 21 and 25 subpulses). The plot suggests that either the pulse separation increases very rapidly toward lower frequencies, or the subpulse detected at 26.3 and 25 MHz is a new one which appears only at low frequencies. In figure 3-9 the average pulse profile obtained in this thesis is compared with that obtained by Bruck and Ustimenko. The phase of the

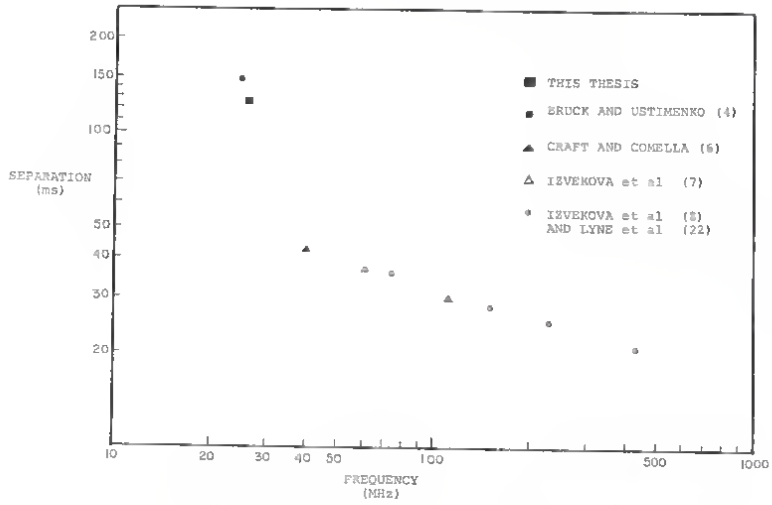

Figure 3-8: Subpulse separation as a function of frequency for the pulsar PSR1133+16

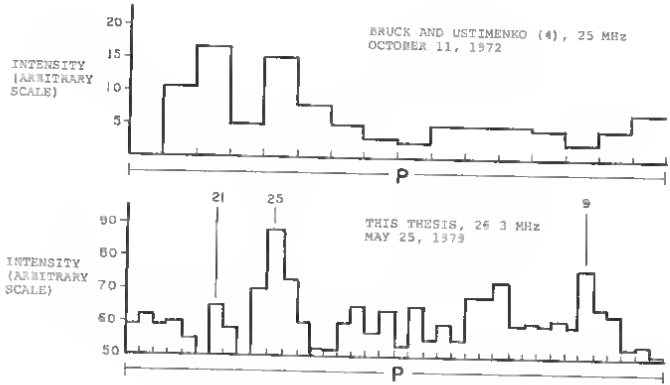

Figure 3-9. Comparison of the pulse profile for pulsar PSR1133+16 obtained in this thesis (average of 340 periods) with that obtained by Bruck and Ustimenko (4) (average of ~212 periods). The bins of the 26.3 MHz pulse profile have been shifted in order to align the pulses.

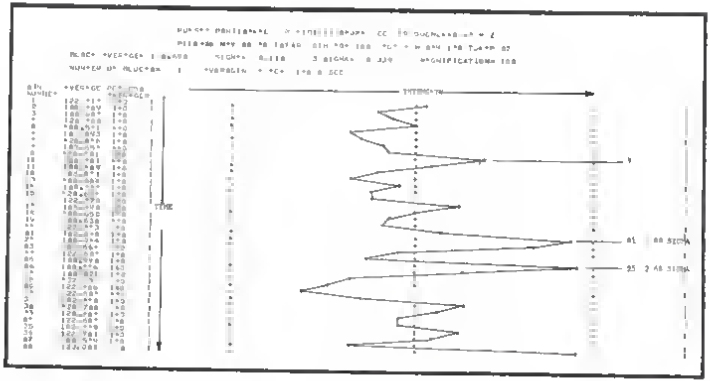

Figure 3-10. Pulsar PSR1133+16 (Block P112WA6) recorded at 26.3 MHz on May 25, 1979. Average over 140 periods.

pulse profile at 26.3 MHz has been shifted [illegible] the pulses in bin 21 and 25 with the pulses at 25 MHz.

Although the subpulse in bin 21 is much weaker than that in bin 25 for the 390-period average, the two are almost the same strength in the 140-period average shown in figure 3-10 (block P112EA6). In the latter case, the heights are 2.68 σ and 2.62 σ for the bin 25 and 21 pulses, respectively. A possible implication is that the bin 21 pulse varies in intensity much more than does that of bin 25.

A small pulse appears in bin 9, when blocks P112WA6 and P112WW6 are averaged together. This pulse is also present in each block average separately (figure 3-5 and 3-6), suggesting the possible existence of an interpulse leading the main pulse by 0.42 P (or 150°). In Druck and Ustimenko [4] a broad and poorly defined pulse seems to appear at 0.5 P from the main pulse, in the same plot where the double main pulse appears (figure 3-9). So far, no interpulse has been reported for this pulsar.

3.1 a Peak Flux Density, Mean Flux Density and Energy for Pulsar PSR1133+16

Several continuous radio sources were observed in order to calibrate the array, to obtain the minimum detectable flux density, and then to obtain an estimate of the peak flux density for pulsar PSR1133+16.

The radio sources observed and their main parameters are presented in Table 3-1.

Table 3-1 Radio sources used for calibration

Radio Source	R.A.	Declination	Flux Density (Jy)	Antenna Beam Used
3C310	$15^h02.5^m$	26°15'6"	3.2	1W, 2W
3C315	$15^h11\ 7^m$	26°16'8"	1.3	1W, 2W
3C409	$20^h12.2^m$	23°25'15"	3.1	1E
3C433	$21^h21.4^m$	24°54'6"	2.7	1W

Positions and flux densities were taken from the Clark Lake Survey at 26.3 MHz (16). Of these four sources, only 3C409 and 3C433 were used in the calibrations, the 3C310 and 3C315 measurements were discarded because their difference in R.A. is only 8.8^m (corresponding to 2.2°). Since the HPBW of the radiotelescope is 6.0° east-to-west, these two sources cannot be resolved

The parameters of the radiotelescope for observing the calibration sources were

Bandwidth ($\Delta\nu$) = 250 kHz

Time constant (τ) = 1.5 s

Frequency (ν) = 26.3 MHz

The minimum detectable flux density S_{min}, deduced from calibrations using these sources, is presented in Table 3-2.

Table 3-1. S_{min} and Galactic background temperatures deduced from calibrations

Radio Source	S_{min} (Jy)	Galactic background temp °K
3C409	101	38,975
3C433	97	27,840

The galactic background temperature for pulsar PSR1133+16 is:

$$T_{backgr} = 18,514°K$$

All the galactic background temperatures given are actual brightness temperatures, corrected for losses in the antenna.

A Hewlett Packard noise generator was used for the calibrations, and a pair of type 5722 noise diodes served as the standard of comparison for the noise generator. Details of the calibrations are given in Appendix E.

The minimum detectable flux density has the following expression (17):

$$\Delta S_{min} \propto \frac{1}{n\Delta\nu\tau} \times T_{syst} \qquad (3\text{-}1)$$

where n = number of averaged records

$\Delta\nu$ = pre-detection bandwidth of the receiver

τ = post-detection time constant

T_{syst} = system temperature

In this case, the temperature of the system is completely dominated by the galactic background temperature, and in

equation (3-1), it is possible to substitute T_{sys} by

$$T_{sys} \quad T_{galactic\ background}$$

Assigning subscripts p to the pulsar and r to a continuous radio source, it is possible by using equation (3-1), to write two similar expressions, one for the pulsar and the other for the radio source. By dividing one by the other, the following expression can be obtained:

$$\Delta S_{min\ p} = \frac{n_r \Delta\nu_r \tau_r}{n_p \Delta\nu_p \tau_p} \frac{T_p}{T_r} S_{min\ r} K \qquad (3-2)$$

The constant K takes into account that the pulsar signal, instead of being continuous, is being sampled.

Using the values obtained for the pulsar on May 25, 1975:

n_p = 390 periods (453 s)

$\Delta\nu_p$ = 8 kHz

τ_p = 12.5 ms

T_p = 18,514°K

and the values for the radio source of

n_r = 1

$\Delta\nu_r$ = 250 kHz

τ_r = 1.5 s

ΔS_r = 101 Jy

T_r = 38,975°K

the following value is obtained

$S_{min\ p}$ = 149 Jy (considering K = 1).

To obtain the peak flux density of the pulsar, it is necessary to make several assumptions

B. In order to be consistent it has been considered that the value S_{min} for both the continuous source and the pulsar is that which would cause a deflection of 3 σ (i.e., 3 standard deviations) from the mean value of the galactic noise background. The 3 σ criterion was used to determine whether or not a pulsar pulse was present at the end of an integration run.

B. It is assumed that the sample rate is fast enough compared with the post-detection time constant that very little information is lost in this process; then K can be considered $\sqrt{1}$. (Details about sampling rates can be found in Appendix B.)

C. It is assumed that the pulsar signal is unpolarized, as in the calibration source. This is probably not correct; a strong linearly polarized component has been reported (18). The effect of variable Faraday rotation in the terrestrial ionosphere would then be to cause the plane of the linearly polarized component to be oriented (at different times) at any angles from parallel to perpendicular with respect to the antenna dipoles. As a result, if the polarization is actually 100% linear, the value of S_{min} as given by (3-2) may range anywhere from too low by a factor of two to too high by a factor of infinity. Thus, no signal at all would be detected if the linear polarization is perpendicular to the dipoles, while according to (3-2) $S_{min\ p}$ would not be zero

Making these assumptions, once the pulsar reaches a value slightly higher than 3σ at the end of an averaging process, the peak flux density can then be considered equal to S_{min} (calculated for the corresponding number of periods averaged). Therefore,

$$S_{peak\ p} = S_{min\ p} = 150 \text{ Jy}$$

Pulse energy is usually defined as:

$$E_p = \int_0^P S(t)\, dt \qquad (3-3)$$

where P = pulsar period

S(t) = flux density as a function of time

For pulsars with no interpulse, the limits of the integral are restricted to the duration of the pulse (base time duration).

In order to make the computations simpler, it is usually assumed that the pulse has a relatively simple geometrical shape. Izvekova et al. [7] assumed a triangular shape for most pulsars (including PSR1133+16). By looking at the pulse shape obtained on May 25, 1979, one can see that this is a reasonably good approximation, considering only the pulse centered at bin 25.

Using this approximation, the pulse energy in equation (3-3) can be written as:

$$E_p = \frac{1}{2} S_{peak\ p} W_{base} \qquad (3-4)$$

where W_{base} = pulse width at base, corrected for dispersion and receiver time constant.

Substituting the values of

$S_{peak\ p}$ = 150 Jy

W_{base} = 71 ms

the following value for E_p is obtained:

$$E_p = 5.3 \times 10^{-26}\ Jm^{-2}Hz^{-1}$$

The mean flux density of the pulse is defined as

$$S_{mean} = E_p/P \qquad (3\text{-}5)$$

Using the value obtained for E_p and the value for the period P = 1.188 sec, the following value for the mean flux density is obtained:

$$S_{mean} = 4.45\ Jy$$

It is interesting, now, to compare these values with values obtained by other authors.

In 1973, Bruck and Ustimenko (4) observed the same pulsar at frequencies of 16.7, 20 and 25 MHz using a linearly polarized broadband array and reported peak flux densities in the range of 10 to 40 Jy.

In 1968, Drake and Craft (19) observed the same pulsar, using the Arecibo 1000-foot radio telescope at frequencies of 111.5 and 195 Mhz and reported peak flux densities of 150 Jy at 111.5 MHz. Since these observations were made at a much higher frequency, they cannot be directly compared with the one at 26.3 MHz, nevertheless, the value obtained at the two frequencies gives an idea of the order of magnitude for the peak flux densities. A value of 38 Jy can be deduced from the data at 61 MHz given by Izvekova et al. (7).

Regarding the pulse energy and mean flux density, more recently, in 1979, Izvekova et al. (7), have given some results at 61 MHz. They obtained a value for the pulse energy of 0.89×10^{-26} $Jm^{-2}Hz^{-1}$ and a mean flux density of 0.75×10^{-26} Jy, using a linearly polarized antenna.

In 1971, Slee and Hill (9), using a circularly polarized antenna, reported at 80 MHz a value for the pulse energy of 2.2×10^{-26} $Jm^{-2}Hz^{-1}$ for one night (with a median over 6 nights of 1.0×10^{-26} $Jm^{-2}Hz^{-1}$).

It is not easy to compare the values obtained in this thesis with values obtained by other authors, because of the polarization used and the different averaging times (not always given). Nevertheless, the value of pulse energy $E_p = 5.3\times10^{-26}$ $Jm^{-2}Hz^{-1}$ obtained at 26.3 MHz, looks at least comparable with the value of $E_p = 2.2\times10^{-26}$ $Jm^{-2}Hz^{-1}$ obtained at 80 MHz (which also corresponds to a peak flux density of ~110 Jy).

According to Izvekova et al. (7), PSR1133+16 has a maximum in its average spectrum at $\nu_{max} = 100\pm40$ MHz. Kuz'min et al. (20), making simultaneous observations at several frequencies, found that the instantaneous spectrum changes from day to day. For several days it doesn't show a maximum in its spectrum but rather the intensity seems to increase towards lower frequencies.

This can be considered as part of the explanation of why the peak flux density, the mean flux density and the pulse energy obtained at 26.3 MHz are higher than the values

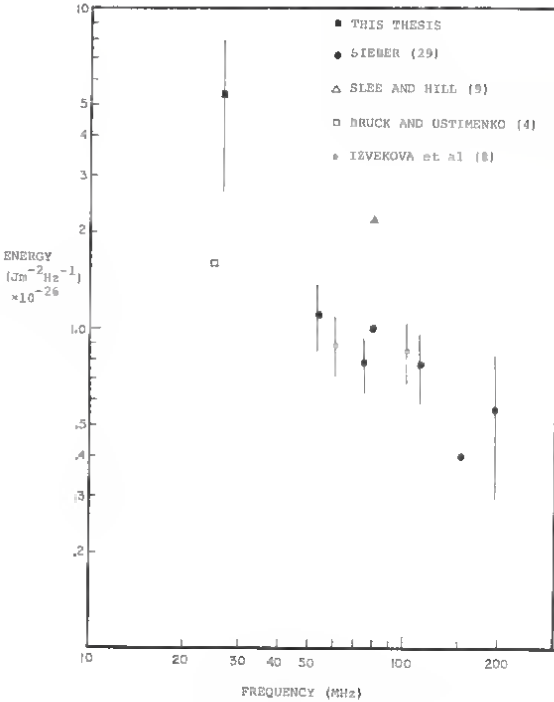

Figure 3-11. Low frequency energy spectrum for pulsar 1^{h}R1133+16

obtained at higher frequencies: the pulsar seems to show abnormally strong pulses at low frequencies during some particular nights, as it may have done in our case.

Another interesting aspect of this has been pointed out by Ekers and Moffet (21). They observed PSR1133+16 at a wave length of 23 cm (~1300 Mhz). From a histogram of energy and number of pulses with a given energy, they noticed a long tail in the distribution, towards the high energy end. The ratio of the mean value (0.020×10^{-26} $Jm^{-2}Hz^{-1}$) to the highest energy pulse ($\sim0.090\times10^{-26}$ $Jm^{-2}Hz^{-1}$) is about 4.5. If one takes the value for the mean energy of $5.3\times10^{-26}Hz^{-1}$ at 26.3 MHz as an average over a relative short period (~390 P), and compares it with the calculated mean energy of 1.6×10^{-26} $Jm^{-2}Hz^{-1}$, obtained from the observations of Bruck and Ustimenko at 25 MHz (4) a value of 3.3 is obtained for the ratio. Such a ratio is not improbable according to the distribution function of Ekers and Moffet. Pulse energies obtained reported in this thesis and by several other authors are plotted as a function of frequency in Figure 3-11.

3.1.b PSR1133+16 Pulse Width

Several factors can distort the actual pulse shape as observed, the factors that need to be considered are:

A. Effect of the dispersion over the finite bandwidth of the receiver.

B. Effect of the post detection time constant of the receiver.

c. Polarization of the pulses and antenna

The first two factors will make the pulse wider than the actual pulse, but their effects can be corrected for if the pre-detection bandwidth, post-detection time constant of the telescope and the dispersion measure for the pulsar are known. A simple form needs also to be assumed for the pulse.

In order to see the effect of dispersion let us consider the basic formula for the time of propagation through a plasma with a dispersion measure DM at a frequency ν. The time of propagation is given by

$$t = kDM \frac{1}{\nu^2} \qquad (3\text{-}6)$$

where k is a constant depending on the plasma

Differentiating this equation with respect to ν, taking finite Δt and $\Delta\nu$ (instead of dt and dν), and expressing the parameters in consistent units, the following expression can be obtained

$$\Delta t = 8.3\times10^{-3} DM\Delta\nu(\nu_o)^{-3} \text{ ms} \qquad (3\text{-}7)$$

where DM - dispersion measure (parsec cm^{-3})

$\Delta\nu$ - bandwidth (kHz)

ν_o = center frequency (hundreds of MHz)

This relationship gives the time it takes for a dispersed pulse to sweep through a bandwidth $\Delta\nu$ centered at frequency ν_o.

If a triangular shape for the pulse is assumed, (3-7) is transformed into (3-8) for the half intensity level

$$\Delta t_{0.5} = 4.15\times10^{-3} DM\Delta\nu(\nu_o)^{-3} \text{ ms} \qquad (3\text{-}8)$$

The correction due to the time constant of the receiver (for the half intensity level and assuming a triangular pulse shape) is given by (8)

$$T_c = 0.693\tau \qquad (3\text{-}9)$$

where τ is the post detection time constant of the receiver

No correction can be made due to the effect of polarization but some discussion about its effect will be given in the conclusions.

Consequently, the corrected half intensity width of the pulse is

$$W_{0.5} = W_{0.5\ ob} - \Delta t_{0.5} - T_c \qquad (3\text{-}10)$$

where $W_{0.5\ ob}$ is the observed half intensity width.

Substituting in equations (3-8) and (3-9) the values

$DM = 4.8$ pc cm^{-3}

$\Delta\nu = 8$ kHz

$\nu_o = 26.3$ MHz

and $\tau = 11.25$ ms,

the following values are obtained for the corrections

$\Delta t_{0.5} = 8.8$ ms

$T_c = 7.8$ ms

Table 3-3 gives the values for the observed half intensity width and the half intensity corrected width for the pulses obtained on April 28 and May 25, 1979. The pulse width at the base is the width assuming a triangular shape, and is twice the corrected half intensity width.

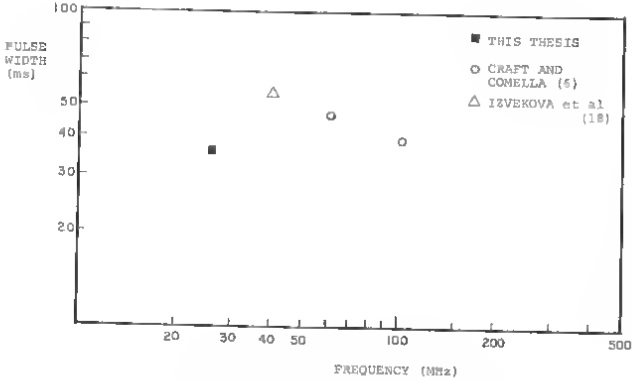

Figure 3-12 Pulsar PSR1133+16 half intensity pulse width as a function of frequency.

Table 3-3. Observed half intensity width, corrected half intensity width, and pulse width at base, for pulsar PSR1133+16

Date	$W_{0.5}$ observed (ms)	$W_{0.5}$ corrected (ms)	W_{base} (ms)
April 28, 1979	38	21	42
May 25, 1979	53	36	72

The graph of Figure 3-12 is a plot of the values of the corrected pulse half-intensity width at several frequencies (6, 8), including the values of this thesis obtained at 26.3 MHz on May 25, 1979; this is the more reliable of the two values presented in Table 3-3.

3.1.c Tests Performed with the Pulse Obtained on May 25, 1979

An independent and simple method for testing the pulses to see if they are indeed from a pulsar having the assumed period is to repeat the averaging process using both shorter and longer periods than that given by the DOPVEL program. If the observed pulses were spurious ones which happened to have approximately (but not exactly) the same period as that of the assumed pulsar, then the averaged intensity should either increase or decrease for the shorter period, and do the opposite for the longer period. If the averaged intensity is a maximum at the assumed pulsar period, then

It is almost [illegible] that the pulse [illegible] to the pulsar

May 25, 1979, the date on which the best pulse was obtained, was chosen to make the test. Data were analyzed using periods longer and shorter than the assumed period by ±40, ±80, ±160, ±320, and ±640 μs.

Periods shorter or longer than the assumed period P by ±80 μs should cause a shift of ±1 bin at the end of the 350 period average.

The result of this test is shown in Figure 3-13, where the relative averaged pulse intensities have been plotted as a function of the assumed period length, taking as the base the period P = 1.188023 s given by the DOPVEL program. It can be seen that the pulse nicely peaks with the assumed pulsar period, and decreases sharply for shorter and longer periods. The lack of symmetry of the plot might be due to the unsymetrical pulse shape.

The computer plots of the results for the different periods used in this test are presented in Figures 3-14 to 3-24.

The pulse intensity as a function of time has been plotted in figure 3-25 for the pulse obtained on May 25, 1979. This pulse was chosen because it was the better of the two and is well defined. This plot is useful not only to visualize the temporal behavior of the intensity of the pulse but also to check that no interference or isolated transient pulse is mistakenly taken as a pulsar pulse.

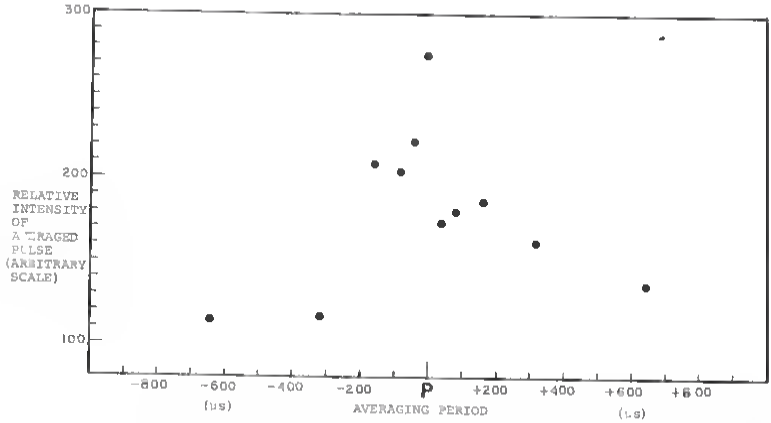

Figure 3-13 Relative pulse intensity as a function of the averaging period for pulsar PSR1133+16 on May 25, 1979 P - 1.188023 s.

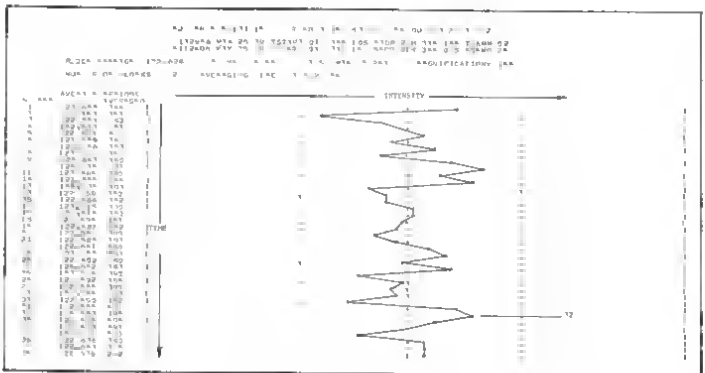

Figure 3-14. Pulsar PSR1133+16 data recorded on May 25, 1975, analyzed with a period P = 1 1B7383 s (P-640 μs).

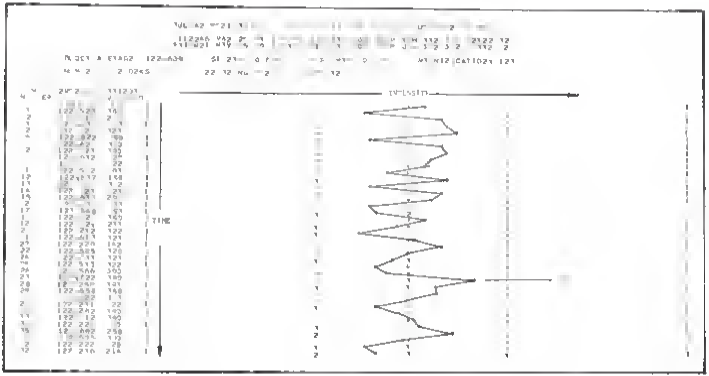

Figure 3-15. Pulsar PSR1133+16 data recorded on May 25, 1979, analyzed with a period P = 1.187702 s (P=320 μs)

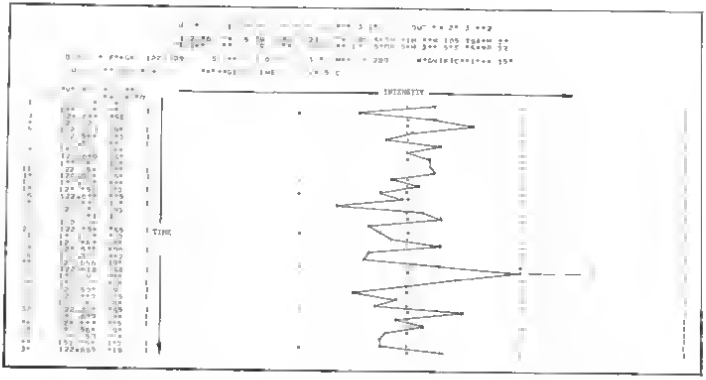

Figure 3-16. Pulsar PSR1133+16 data recorded on May 25, 1979 analyzed with a period P = 1.187863 s (P-160 us)

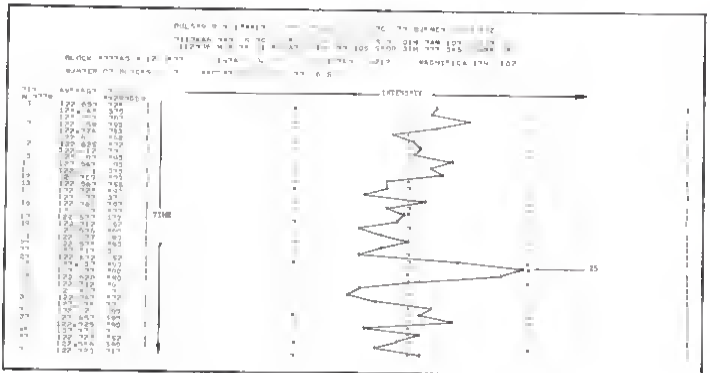

Figure 3-17. Pulsar PSR1133+16 data recorded on May 25, 1979, analyzed with a period P = 1.187943 s (P-80 μs).

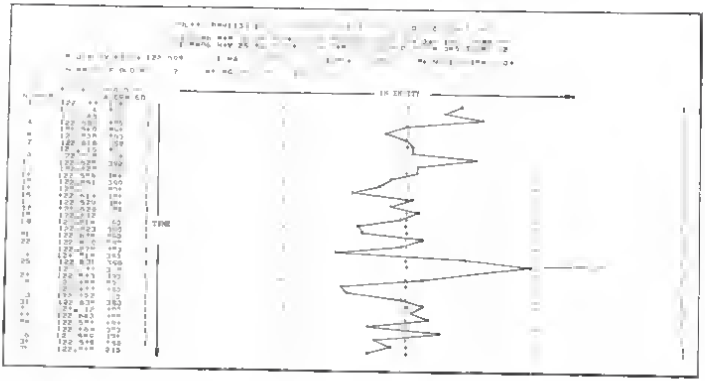

Figure 3-18. Pulsar PSR1133+16 data recorded on May 25, 1979, analyzed with a period P = 1.187983 s (P=40 μs).

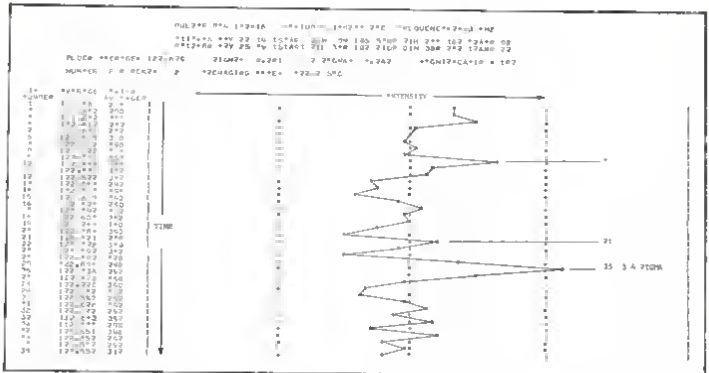

Figure 3-19. Pulsar PSR1133+16 data recorded on May 25, 1979, analyzed with a period P = 1.188023 s (DOPVEL period).

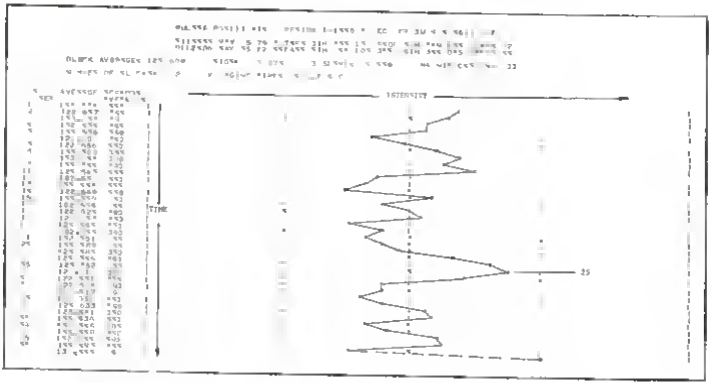

Figure 3-20. Pulsar PSR1133+16 data recorded on May 25, 1979, analyzed with a period P = 1.188063 s (P+40 us).

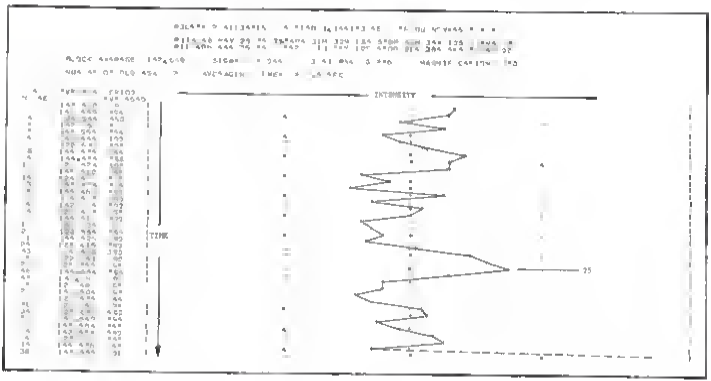

Figure 3-21. Pulsar PSR1133+16 data recorded on May 25, 1979, analyzed with a period P = 1.188103 s (P+80 μs)

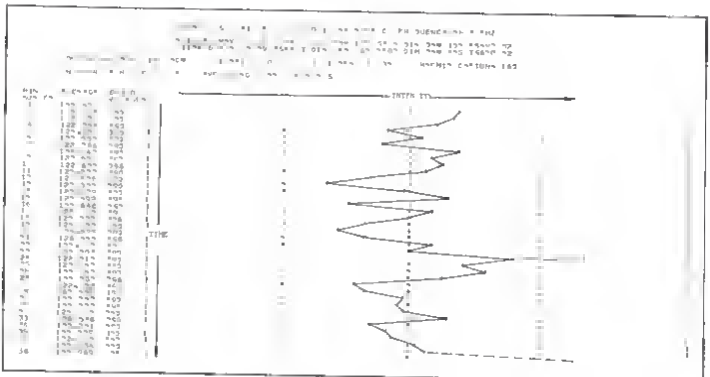

Figure 3-22: Pulsar PSR1133+16 data recorded on May 25, 1979, analyzed with a Period P = 1.188183 s (P+160 μs).

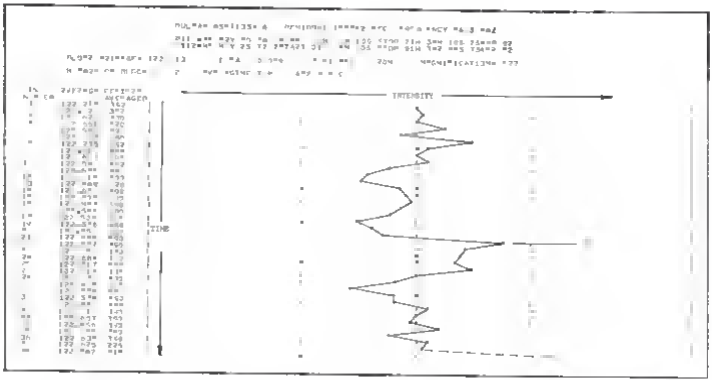

Figure 3-23: Pulsar PSR1133+16 data recorded on May 25, 1979. [illegible] period P = 1.188342 s (P+320 μs).

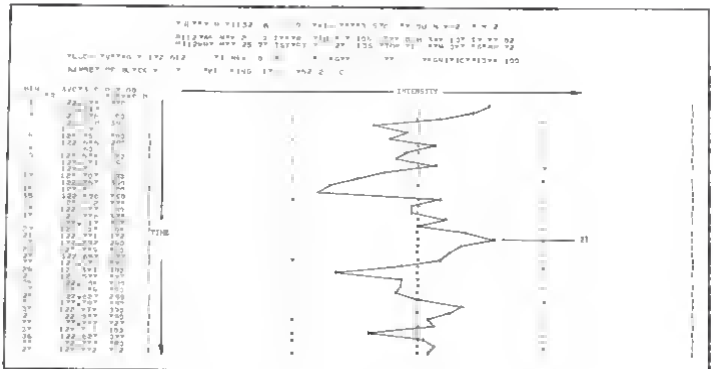

Figure 3-24. Pulsar PSR1133+16 data recorded on May 25, 1979, analyzed with a period P = 1.188553 s (P+640 μs).

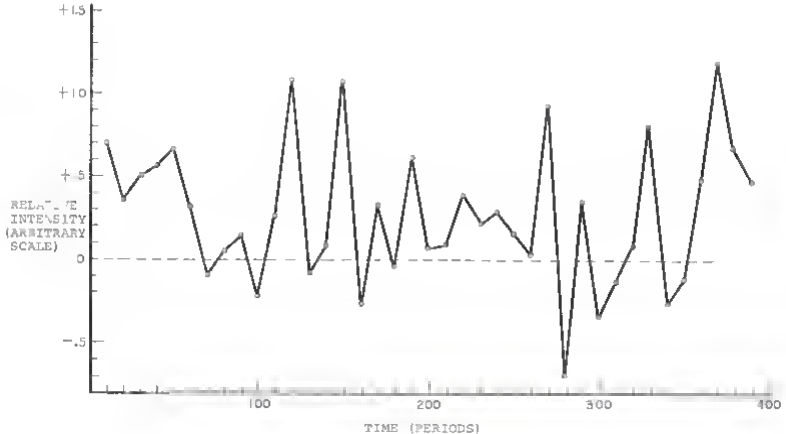

Figure 3-25 Relative pulse intensity as a function of time (periods) for pulsar PSR1133+16 on May 15, 1979. Each point represents an average over 10 periods. P = 1.18#023 s.

It can be regarded as a double check of the [illegible] described.

Each point on the graph represents the intensity with respect to its corresponding average value of 10 consecutive periods, for bin 25 (peak of the pulse at the end of the averaging process). The intensity scale is in arbitrary units and the time scale is in periods P given by the DOPVEL program (P = 1.188023 s). The plot shows that the intensity in bin 25 is almost always positive with respect to its corresponding 10-periods average value, and no clear periodic variations appear over the 390 periods plotted.

3.2 PSR2045-16 Data Analysis

Of the 10 nights of data reduced for pulsar PSR2045-16, pulses were found on 4 nights: May 15, 16, 18 and 19, 1979.

A summary of the dates, averaged pulse deflection in terms of standard deviations σ, and number of periods averaged is presented in Table 3-4.

Table 3-4: Summary of the date, pulse deflection and number of periods averaged each night for pulsar PSR2045-16

Date	Pulse deflection in terms of σ	Periods averaged
May 15, 1979	3.16	540
May 16, 1979	3.48	440
May 18, 1979	3.28	610
May 19, 1979	3.30	415

Plots of the data for these dates are presented in Figures 3-26 to 3-30. Figure 3-31 corresponds to a plot of a typical day when only noise was present and no pulse appeared.

In general the pulses were of different shapes, except for the last two days, for which the shapes were similar. Some have steep leading and trailing edges (as on May 16, Figure 3-28); others have only a steep trailing edge and a not so well defined leading edge (as on May 15, Figure 3-26). On May 18 and 19 (Figures 3-29 and 3-30) both pulses show a steep leading edge and much less steep trailing edge.

On May 16 the pulse was clearly present with an intensity of 3.48 σ above the mean value over an average of only 180 periods (Figure 3-27). On the other 3 days, pulses were not seen clearly until the end of the averaging process for that night. For partial averages in these cases, some indication of a pulse can be seen at the location where the pulse appears after completing the average, but its intensity never rises significantly above the noise level. No indication of the existence of a complex pulse or interpulse can be deduced from the plotted data.

Pulsar PSR2045-16 presents at higher frequencies a complex pulse, composed of 3 subpulses, with the trailing subpulse decreasing dramatically in intensity with decreasing frequency (22); at 610 MHz the trailing pulse

Figure 1. [illegible] recorded on Nov. 15, 1979, at 45 MHz. [illegible]

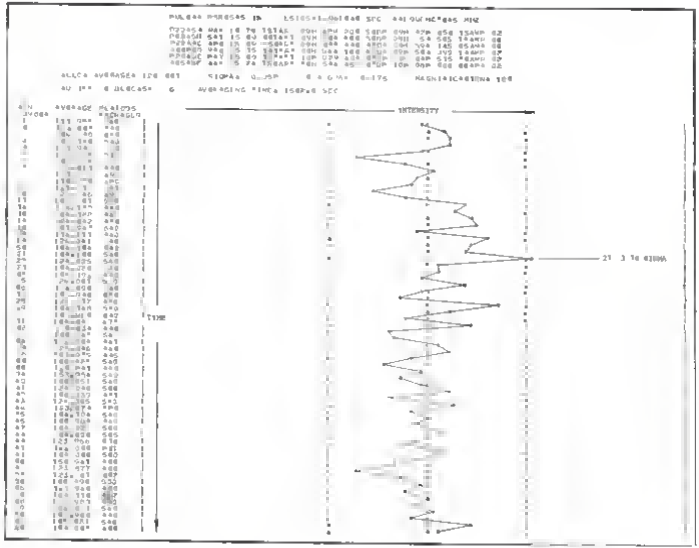
INTENSITY
TIME

Figure [illegible] Pulsar PSR2045-16 recorded on May 15, 1979, a[illegible] average over 180 periods.

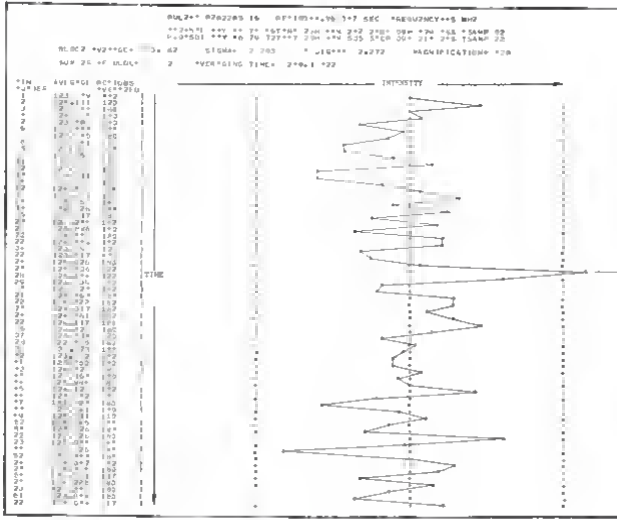
INTENSITY
TIME
27
3 AR
SIGMA

Figure 3-28. Pulsar PSR2045-16 recorded on May [illegible]
Average over 440 periods.

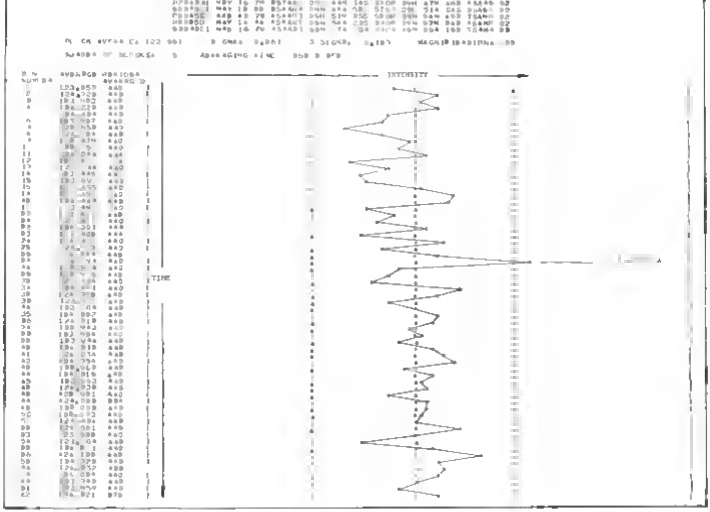
INTENSITY
TIME

Figure 3-29. Pulsar PSR2045-16 recorded on [illegible]
Average over 610 periods.

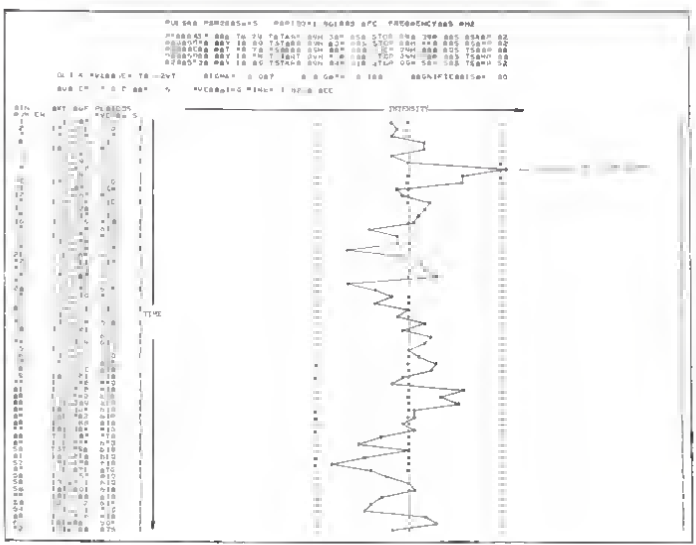
INTENSITY
TIME

Figure 3.30. Pulsar PSR2045-16 recorded on [illegible] 19, 1979, at 45 MHz
Average over 415 periods.

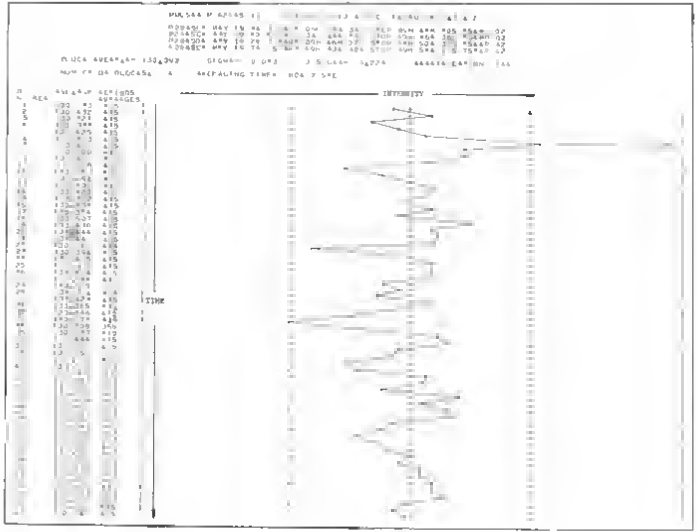
INTENSITY
TIME

Figure 1-21 Pulsar PSR2045-16 recorded on May 17, 1979, at 45 MHz. Average over 390 periods. No pulse present

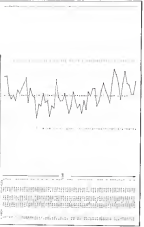

is the most intense, but the intensity decreases rapidly, and at 151 MHz is about 2/3 of the central subpulse. The intensity of the central and leading subpulses seems to remain almost constant with frequency. No indication of resolved subpulses can be obtained from the data at 45 MHz. Nevertheless, the difference in steepness of the leading and trailing edges might suggest the existence of an unresolved much less intense subpulse accompanying the main subpulse. This aspect will be discussed later when discussing the pulse width and the effect of polarization.

3.2.a Peak Flux Density, Mean Flux Density and Energy for Pulsar PSR2045-16

In order to estimate the peak flux density of this pulsar, several radio sources were observed for calibration purposes. Radio source PKS2034-17, one of the closest to the pulsar, was clearly recorded despite the steepness of the galactic background (23). This radio source has apparently not been observed before at any frequency lower than 80 MHz. However, an extrapolated flux density at 45 MHz was obtained from the spectral index derived from flux density data at higher frequencies, as reported in the literature.

Spectral index can be defined (17) by the relation:

$$S \propto \left(\frac{1}{\nu}\right)^{n} \qquad (3\text{-}11)$$

where S = flux density

ν = frequency

n = spectral index

For any two frequencies on the linear part of the relationship between S and $\frac{1}{\nu}$,

$$\frac{S_{\nu 1}}{S_{\nu 2}} = \left(\frac{\nu_2}{\nu_1} \right)^n$$

The best available values of the flux density for this source (24, 25) are at frequencies of 160 and 80 MHz

$$S_{160} = 8.8 \text{ Jy}$$

$$S_{80} = 15 \text{ Jy}$$

Substituting these values into equation (3-12), a value of n = 0.76 is obtained

Assuming a linear relationship for S as a function of $\frac{1}{\nu}$ down to 45 MHz, the flux density at this frequency is found to be

$$S_{45} = 23 \text{ Jy}$$

Applying the previously used criteria, the following value for the minimum detectable flux density at 45 MHz was obtained for the region near source PKS2045-17.

$$S_{min} = 6 \text{ Jy}$$

The radiotelescope parameters for observing the radio source PKS2045-17 were

$$\Delta\nu = 3 \text{ MHz}$$

$$\tau = 3 \text{ S}$$

$$n_r = 1$$

where $\Delta\nu$ = bandwidth, τ = post detection [illegible]
and n_r = number of records averaged

It can be shown that the brightness temperature T and the frequency ν are related in a similar way as S and ν are related in equation (3-12)

$$\frac{T_{\nu 1}}{T_{\nu 2}} = \left(\frac{\nu_2}{\nu_1}\right)^n \qquad (3\text{-}13)$$

Using the galactic background temperature at 38 MHz given by Blythe (26):

$$T_p = 12{,}000°K$$

$$T_r = 7{,}000°K$$

where T_p = galactic background temperature near the pulsar

T_r = galactic background temperature near the radio source PKS2034-17

and the value for the galactic background spectral index given by Findlay (27), valid for the range 20 to 400 MHz

$$n = 2.65$$

the galactic background temperatures T_p and T_r at 45 MHz were found to be,

$$T_p = 7{,}630°K$$

$$T_r = 4{,}452°K$$

Using equation (3-2) and the appropriate parameters of the radio telescope, the minimum detectable flux density can be obtained for the pulsar observations.

The radi[illegible] parameters wh[illegible]erving PSR2034-17 are:

$\Delta\nu_r$ = 3 MHz

τ_r = 3 s

n_r = 1

T_r = 4,452°K

S_{min} = 8 Jy

The parameters when observing the pulsar are:

$\Delta\nu_p$ = 10 kHz

τ_p = 11.25 ms

n_p = variable, depends on the day

T_p = 7,630°K

The peak flux density (which is also the minimum detectable flux density) for the different days is shown in Table 3-5; this table also contains the values of the mean pulse energy and mean flux density computed using equations (3-4), (3-5) and the values for the pulse width given in Table 3-6.

No known measurements of flux density and energy at low radiofrequencies exist for pulsar PSR2045-16. The lowest frequency data on this pulsar are the 80 MHz observations made by Slee and Hill [9]. They attempted to observe the pulsar on 3 nights, failing to detect it and giving an upper limit for the pulse energy of $<0.17\times10^{-26}$ $Jm^{-2}Hz^{-1}$. The failure to detect this pulsar is not surprising since it has been reported to have large

Table 3-5 Summary of Peak flux densities, Mean Pulse energies and Mean flux densities for Pulsar PSR2045-16 at 45 MHz.

Date	Periods Averaged	Peak Flux Density Jy	Mean Pulse Energy $Jm^{-2}Hz^{-1}$	Mean Flux Density
May 15, 1979	540	125	3.8	1.95
May 16, 1979	440	139	3.4	1.73
May 18, 1979	610	118	3.5	1.8
May 19, 1979	415	143	4.4	2.25
		Unweighted Mean	3.775	

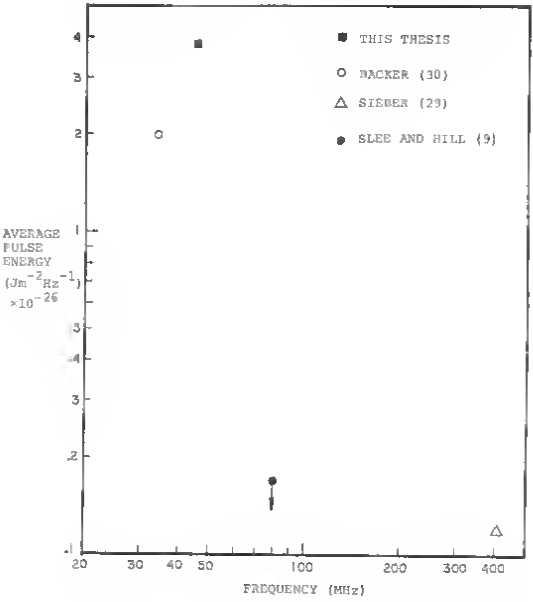

Figure 3-32 Pulsar PSR2045-16 low frequency energy spectrum.

intensity variations being often undetectable (28, 29). Our experiences at 45 MHz confirm this behavior also since it was possible to detect this pulsar only in the first nights of the observing period; it faded out for the rest of the nights.

An unconfirmed pulse energy of $\sim 1.9\ Jm^{-2}Hz^{-1}$ has been given by Backer at 34 MHz (30). The lowest frequency at which published data on pulse energy is available is 410 MHz; the energy is $0.120\times10^{-26}\ Jm^{-2}Hz^{-1}$ (29, 31). Our measurement at 45 MHz seems rather high (perhaps suggesting an undetected systematic error), although no direct comparison is possible due to the lack of published information at low frequencies on this pulsar.

Pulse energy as a function of the frequency has been plotted in Figure 3-32, including the data mentioned in the last paragraphs.

3.2.b Pulse Width for Pulsar PSR2045-16

In order to obtain the true half intensity pulse width of PSR2045-16 at 45 MHz, the measured half intensity pulse width has been corrected for pulse dispersion and post detection time constant using equations (3-8) and (3-9) respectively.

In order to correct for pulse dispersion, the following values for the parameters were used:

$\Delta\nu$ = 10 kHz

ν_o = 45 MHz

DM = 11.5 pc cm^{-3}

The correction for pulse dis[illegible] the above values, is

$$\Delta t_{0.5} = 10.5 \text{ ms}$$

The correction due to the post detection time constant of $\tau_c = 11.25$ ms is,

$$T_c = 7.8 \text{ ms}$$

The true (or corrected) half intensity pulse width $W_{0.5}$ is as before (equation 3-10)

$$W_{0.5} = W_{0.5 \text{ obs}} - \Delta t_{0.5} - T_c$$

The result for the 4 days is shown in Table 3-6

Table 3-6: Observed and corrected half intensity pulse width and pulse width at base (assuming triangular shape).

Date	$W_{0.5 \text{ obs}}$ (ms)	$W_{0.5}$ (ms)	Width at base (ms)
May 15, 1979	44	31	62
May 16, 1979	38	25	50
May 18, 1979	44	31	62
May 19, 1979	44	31	62

The lowest frequencies at which pulse shape and width measurements have been given for this pulsar are 150 and 151 MHz (10, 22). Lyne et al. (22) have given the separation between subpulses at a number of frequencies, the values are plotted in Figure 3-33. The separation between

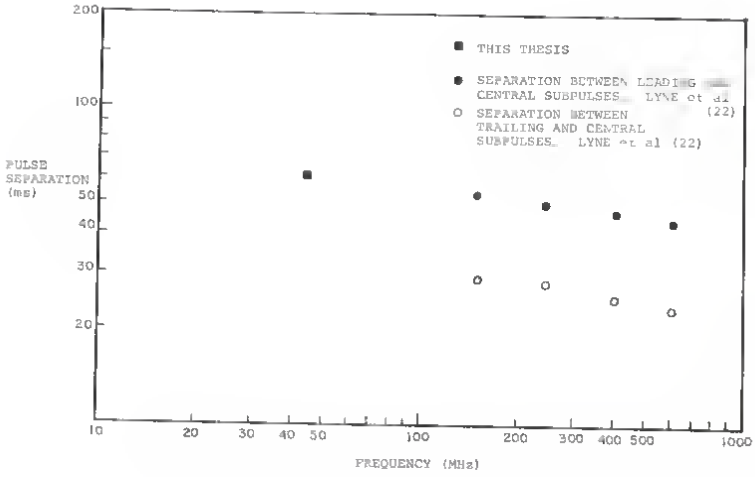

Figure 3-33 Pulsar PSR2045-16 subpulse separation as a function of frequency, including the pulse width at the base obtained at 45 MHz in this thesis.

the leading and central subpulses and the trailing and central subpulses is plotted separately

As in a previously mentioned case, the trailing pulse seems to decrease very rapidly in intensity toward lower frequencies (22), and it is likely that at 45 MHz it no longer exists or at least it can be very weak. The mean value at 45 MHz for the pulse width at its base (obtained by measuring the width at half intensity and assuming a triangular shape) of 61 ms has also been plotted in Figure 3-33.

The plotted value for the pulse width at its base, lies close to the extrapolation of a straight line passing through the points representing the separation between the leading and central subpulses. A possible conclusion of this is that the pulse observed at 45 MHz is composed of two unresolved pulses which might correspond to the leading and central subpulses at higher frequencies; the pulse width at its base would correspond to the separation between the two subpulses

No polarization measurements have been made for this pulsar at low frequency. The lowest frequency at which polarization measurements are available is 409 MHz (32, 33) The mean percentage of linear polarization at 409 MHz is 40%, and it changes during the course of the pulse, reaching about 70% for the first subpulse. The stability of the linear polarization position angle is low for the wings of the integrated pulse profile, due to the occasional

occurrence of pulses with orthogonal polarization with respect to the mean, but is high at the center of the pulse (32). If the degree of linear polarization of the pulse is higher at lower frequencies, there will probably be a distortion in the pulse shape when it is received with a linearly polarized antenna. This distortion will depend on the variation of the polarization angle within the pulse. Assuming that the linearly polarized component in the central part of the pulse is parallel (or nearly parallel) to the antenna, then the integrated pulse profile will appear strong in the center; however the slopes of the leading and trailing edges will be weaker and the averaged pulse profile will be narrow. More details about the effect of the degree of linearly polarized component on the pulse profile and apparent intensity variations are given in the conclusions.

3.2.c Period of Pulsar PSR2045-16 from Observations on Two Consecutive Days

The apparent mean pulse period of a pulsar can be calculated from the elapsed time between two pulses, in order to increase the accuracy it is desirable that the elapsed time between the two pulses be much longer than the pulsar period. An attempt was made to obtain the apparent mean pulse period from observations made 24^h apart (elapsed time $\sim 24^h$) for pulsar PSR2045-16. On two occasions the pulsar was detected on two consecutive days,

the first occasion was May 15 and 16, 1979, and the second May 18 and 19, 1979.

The pulse period can be obtained by subtracting the epoch of apparition of the pulse E on two consecutive days and dividing by an integer number N.

The epoch of the pulse can be calculated from the relationship:

$$E = T_{start} + n \times R \qquad (3\text{-}14)$$

where:

T_{start} = time start digitizing

n = bin number where the pulse occurs

R = plotting time resolution

The information related to the two pairs of days has been summarized in Table 3-7

The mean apparent period can be calculated from the relationship

$$P = \frac{\Delta E}{N} \qquad (3\text{-}15)$$

where ΔE: difference in epoch of pulse apparition on two consecutive days (elapsed time between pulse apparitions)

The mean apparent periods obtained with this method are compared with the DOPVEL periods in Table 3-8.

Table 3-7 Epoch and [illegible] PSR2045-16

Date	n	R (s)	I	ΔE (s)	k
May 15, 1979	27	0.0316	$09^h\ 43^m\ 20^s.66434$	[illegible]	[illegible]
May 16, 1979	8	0.0316	$09^h\ 44^m\ 34^s.85415$		
May 18, 1979	8	0.0316	$09^h\ 38^m\ 00^s.25308$	$86189^s.9367$	43944 or 43943
May 19, 1979	6	0.0316	$09^h\ 34^m\ 30^s.18981$		

Table III. Comparison of the mean apparent pulsar periods for PSR2045-16 obtained from observations with the DOPVEL periods.

Date	Mean apparent period (s)	DOPVEL period (s)	ΔP (μs)
May 15, 1979	1.96137547	1.9613783	-6
May 16, 1979			
May 18, 1979	1.96135847	1.9613786	-28
May 19, 1979	or 1.96140311		+14

It can be seen that the periods do not agree. Unfortunately, a jump in the epoch was noticed in the quartz time standard of Malpu, after the first pair of days, that makes the figures for the last pair of days (May 18 and May 19, 1979) very unreliable.

In any case, this discrepancy, at least for May 15 and May 16, demonstrates that the DOPVEL period cannot be used to bring in phase two consecutive days of observations.

In order to bring in phase pulses detected on two consecutive days (within ±0.5 bin), the apparent mean period for each day needs to be known with an accuracy of at least

$$A_c = \left(\frac{P}{2}\right)/N \qquad (3\text{-}16)$$

where N = integer number of periods between two apparitions.

Expressed in terms of the elapsed time T and the period P, (3-16) becomes:

$$A_c = \frac{P}{2}\times\frac{P}{T} \qquad (3\text{-}17)$$

where $N = \frac{T}{P}$

Assuming an elapsed time of 24^h (=86400 s), a resolution of 0.0315 s and a period of 1.961386 s, the following accuracy for the period is obtained:

$$A_c = 0.36\ \mu s$$

This accuracy should bring the two pulses in phase within ±0.5 bin.

It is not clear what caused the discrepancies between the DOPVEL period and the period deduced from the observations; it could be an instrumental problem or a precision problem in the calculations in the DOPVEL program. Both possibilities were checked but the result was inconclusive, further investigations need to be made.

3.2 d Pulsar PSR2045-16 Pulse Intensity as Function of Time

Figure 3-34 is a plot of the relative pulse intensity as a function of time for the pulse obtained on May 16, 1979; this pulse is the strongest and best defined. Each point plotted represents the relative intensity with respect to the noise average, averaged over 10 periods; the time axis scale is in pulsar periods. It can be seen that the pulse has large intensity variations. Most of the time it has a positive value with respect to the noise average, and it seems to show an almost periodic intensity modulation of ~140 periods (peaks at periods 20, 160 and 320).

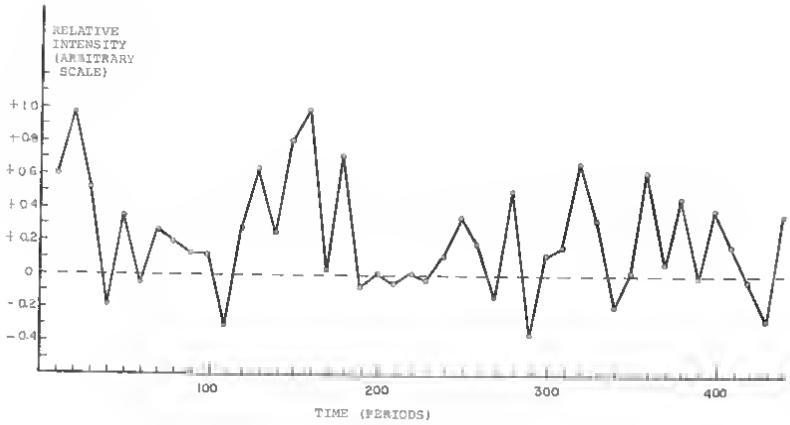

Figure 3-34. Relative pulse intensity as a function of time (periods) for pulsar PSR2045-16 on May 16, 1979. Each point represents an average of 10 periods. P = 1.961383 s.

CHAPTER 4
CONCLUSIONS

Two pulsars have been successfully detected using narrow bandwidth and long averaging times. Pulsar PSR1133+16 was detected with the University of Florida large array at 26.3 MHz and pulsar PSR2045-16 was detected using the Maipu Radio Observatory large array at 45 MHz. Pulsar PSR1133+16 was strong enough to be considered statistically significant (pulse deflection larger than 3 standard deviations) in the data of 2 nights (out of 10 nights reduced). Pulses of PSR2045-16 were found on 4 nights (out of 10 reduced) with enough intensity to reach the 3 standard deviation level. Typical averaging times for both pulsars were in the range 400 to 600 periods.

Both pulsars show large intensity variations on a time scale of days. Typically, one would appear after an averaging time as short as ~200 periods, and then would fade, being undetectable for averaging times as long as ~1500 periods over succeeding days.

The peak pulse flux density obtained for PSR1133+16 is about 150 Jy, for PSR2045-16 the peak flux density is in the range of 120 to 140 Jy. These values (which have relatively large probable error, in the order of 50%), are higher than the values of the peak flux density measured by others at

nearby frequencies. They are also larger than the extrapolated flux densities from published data at higher frequencies.

Also, the pulse shape and half intensity width seem to differ from extrapolated values based on data at higher frequencies.

In order to find a satisfactory explanation of the intensity variations of the two pulsars, it is necessary to consider both previously reported intensity variations and the data available on polarization at higher frequencies.

Pulsar PSR1133+16 and several other pulsars have been reported to show extremely variable flux densities both from pulse to pulse and on a longer time scale, when observed at 81.5 MHz (34). These intensity variations are not believed to be caused by interplanetary scintillation, and therefore must be attributed to the source.

Pulsar PSR2045-16 has been reported as often being undetectable for several days at 408 MHz, but when it is active it can produce pulses stronger than any other of the first pulsars discovered (28).

Besides these intensity variations, the intensity of the received signal will show larger and more frequent variations when received by a linearly polarized antenna, if the pulses are strongly linearly polarized. Manchester et al. have found that most pulsars present a relatively high degree of linear polarization (32). PSR1133+16 was found to have a degree of linear polarization of 33% at

403 MHz, 50% at 86 MHz and 60% at 63 MHz, which is the lowest frequency at which polarization has been measured for this pulsar (35, 36). There is a clear dependence of percentage of linear polarization upon wavelength, and the tendency is for the percentage of linear polarization to increase with increasing wavelength. Pulsar PSR1133+16 has a complex pulse, composed of two subpulses; the percentage of linear polarization is variable throughout the pulse and reaches about 70% in the middle of it at 403 MHz. For individual pulses, the position angle of the plane of linear polarization is highly stable for all but the first component, which usually shows two preferred positions perpendicular to each other. The result of this is that the degree of linear polarization of the integrated pulse is low for the first subpulse and high for the rest (32).

Pulsar PSR2045-16 has a complex pulse composed of 3 subpulses. Manchester et al. (32) measured the degree of linear polarization to be 40% at 403 MHz, with the polarization being even larger for the first subpulse (~70%). The position angle of the plane of linear polarization varies smoothly throughout the pulse; a change of about 30° occurs between the first and third subpulses. This pattern of position angle variation within a pulse is stable for many consecutive pulses. No known polarization measurements are available at lower frequencies for this pulsar.

Even if the linear polarization position angle were stable when measured at a point above the terrestrial

ionosphere, the ionosphere can introduce relatively large variations in the angle as measured at ground level. This is due to variations in the amount of Faraday rotation in the ionosphere. This effect is particularly strong at longer wavelengths because the angle of rotation Ψ is proportional to the square of the wavelength λ

$$\Psi = RM \cdot \lambda^2 \qquad (4\text{-}1)$$

where RM = rotation measure of the ionospheric path.

The RM depends linearly on the electron density, N, the component of the earth's magnetic field intensity which is parallel to the direction of propagation, $B_{\parallel}$, and the thickness of the ionosphere, L:

$$RM = \int_0^L B_{\parallel} N dL \qquad (4\text{-}2)$$

It can be shown that the percent variation of Ψ is equal to the percent variation of the electron density N, if the thickness L and the magnetic field $B_{\parallel}$ of the ionosphere remain constant; that is:

$$\frac{\Delta\Psi}{\Psi}\ \% = \frac{\Delta N}{N}\ \% \qquad (4\text{-}3)$$

It can also be shown that $\frac{\Delta\Psi}{\Psi}$ equals $\frac{\Delta L}{L}$ when N and $B_{\parallel}$ are constant, and equals $\frac{\Delta B_{\parallel}}{B_{\parallel}}$ when N and L are constant.

Manchester has obtained values of ionospheric RM ranging from 0.1 to 6 rad m^{-2}, depending on the time of day and the declination of the pulsars (37). Taking these two extreme values, it is possible to obtain the change in rotation angle, $\Delta\Psi$, for let us say, a 1% change in ΔN at

both 26 3 and 45 MHz. The result of this calculation is shown in Table 4-1

Table 4-1: Variation of the position angle $\Delta\theta$ due to variations of 1% in ΔN, $\Delta B_{\parallel}$ or ΔL in the ionosphere.

Frequency (MHz)	$\Delta\theta$ for $\frac{\Delta N}{N}$, $\frac{\Delta B_{\parallel}}{B_{\parallel}}$ or $\frac{\Delta L}{L}$ = 1%, and RM = 0.1 rad m^{-2}	$\Delta\theta$ for $\frac{\Delta N}{N}$, $\frac{\Delta B_{\parallel}}{B_{\parallel}}$ or $\frac{\Delta L}{L}$ = 1%, and RM = 6 rad m^{-2}
26 3	7.4°	447°
45	2.5°	150°

From the values obtained in Table 4-1, one should expect large random (or nearly random) variations of the position angle for large values of RM at the two frequencies considered This effect could produce a modulation which distorts the pulse shape, in addition to the long term intensity variations. For low and medium values of RM, the variations of the rotation angle $\Delta\theta$ are not so important, since they are small. There is another effect that can be important for large values of RM that is the change in position angle when observing the pulsar in different regions of the sky (i e. when observing the pulsar with different beams), or when observing the pulsar on different nights For example, at 45 MHz, with a RM = 1 rad m^{-2}, a change of 4% of N, L or $B_{\parallel}$ (or a combination of them), will cause the position angle to be orthogonal to its previous position. If the pulsar

radiation is relatively highly linearly polarized [illegible] should produce a significant drop in the intensity of the received signal when using a linearly polarized antenna. This last effect can provide a possible explanation of the disappearance of the pulsar signal when switching to a different beam of the 26.3 MHz array.

Regarding the effect of the polarization throughout the pulse, the pulse shape can be modified when using a linearly polarized antenna; the signal will appear more intense for the part of the pulse with polarization that matches the polarization of the antenna, and abnormally weak for the part of the pulse with position angle unfavorable for the antenna. Also if a given part of the pulse presents random changes in the position angle from normal to orthogonal (which led to a low integrated polarization for that part of the pulse), the intensity of the averaged pulse will be abnormally weak in that part. This seems to be the case with PSR1133+16, in which the observed intensity at 26.3 MHz of the second subpulse is usually stronger than the intensity of the first subpulse, the latter is often undetectable or appears only occasionally. The separation of these two subpulses at 26.3 MHz is much larger (~125 ms) than the predicted separation for the two subpulses (which compose the main pulse) obtained from data at higher frequencies, however the separation at 26.3 MHz does agree with the results obtained at 25 MHz [4].

The values for the peak flux density, the mean flux density and the mean energy are higher than the values obtained from extrapolation at higher frequencies, with the exception of a value of peak flux density of 150 Jy obtained at the relatively high frequency of 111.5 MHz for PSR1133+16. Izvekova et al. (7) and Kuz'min et al. (20) made simultaneous observations of this pulsar at several frequencies in order to obtain the spectrum. They found that the average spectrum (average over several nights) presents a turn-over at about 60 MHz. Nevertheless they also found that the spectrum shows large variations from day to day in the range 61 - 151 MHz, often with a change in the sign of the spectral index. It is interesting to note that the spectrum of some individual nights does not show a turn-over but rather an increasing intensity with decreasing frequencies. This might explain (at least in part) the unusually large intensity of the pulses at 26.3 MHz, when compared with average values obtained by other authors at higher frequencies.

Averaging of pulses for two different nights was not possible. For pulsar PSR2045-16, the period obtained from the DOPVEL program differs from the period deduced from observations on two consecutive nights by amounts between 8 to 28 μs; this discrepancy is large compared with the required precision for averaging over two consecutive days (i.e., ∿ tenths of μs). No attempt was made for PSR1133+16 to average data of two different nights since the only two

nights with data are 27 days apart. It is not clear up to the present whether the discrepancy of the periods is due to instrumental problems or insufficient precision in the calculations of the predicted period.

From the results obtained in this thesis, it has been shown that it is possible to detect pulsars at both 26.3 MHz and 45 MHz, with certain limitations. In the light of the results obtained, some improvements and modifications in the equipment and data reduction can be suggested which will make it possible to obtain even more information about the received emission.

One such modification is already being put into effect. A greatly improved transistorized 26.3 MHz receiver which will replace the old receiver is under construction and is nearly completed.

Recording at a much wider bandwidth (perhaps 50-100 kHz), and utilizing a de-dispersion technique, would considerably increase the signal-to-noise ratio. The wide band signal would initially be recorded using an instrumental tape recorder of suitable bandwidth. It could then be played back into the Saicor Real Time Spectrum Analyzer, the output of which could be digitized and further analyzed by means of a microprocessor or a minicomputer (like the PDP 1134). After the data has been converted to a power spectrum appearing in the 200 output frequency channels of the Saicor spectrum analyzer, the frequency dispersion can then be removed by means of the computer. With a 100 kHz-bandwidth

system of this type, the signal-to-noise ratio would be increased by a factor of $\sqrt{\frac{100}{8}}$, or 3 5, over what it was with the 8 kHz-bandwidth system.

Another advantage of a wide bandwidth system, and perhaps an even more important one, is its ability to determine the degree of linear polarization of the pulsar signals by making use of Faraday rotation in the terrestrial ionosphere. As stated previously, the rotation of the plane of linear polarization varies, due both to ionospheric fluctuations and to a continual change in the ray path as the earth rotates, so that the polarization plane is frequently parallel and frequently perpendicular to the antenna dipoles The degree of linear polarization is readily calculable from the measured intensities at times of parallel and perpendicular orientations. This appears to be an excellent method for determining linear polarization it has apparently not previously been used for pulsars

Also, if the rotation measure (RM) of the ionosphere above the observatory can be determined independently, the position angle of the plane of linear polarization of the pulsar signal at the top of the ionosphere can be calculated.

It may also be possible to obtain still more information about polarization Since the dipoles of the 26.3 MHz array in the Dixie County radio observatory have the capability to be rotated to any position, half of the array can be rotated in 90° respect to the remaining half, making possible to obtain information about the circularly

polarized component of the emission. If for some pulses there is enough signal-to-noise ratio, it would also be possible to set the antenna in such a way that one third of the array is oriented at 0°, one third at 45° and the last third at 90°, from the information obtained in this configuration it is possible to deduce the Stokes parameters of the incident wave. Any pulsar polarization measurement made at 26.3 MHz and 45 MHz would be useful since none have been made at frequencies lower than 63 MHz (36).

Improvements need to be made in the calibrations in order to obtain more accurate values for the peak flux density. This can be accomplished by simulating the pulsar pulse using a precise time standard and a frequency synthesizer, in order to obtain periods within some μ seconds of the observed period. It should be possible to obtain estimations of peak flux densities by digitizing and processing this signal in a similar manner to the actual pulsar. It will be also necessary to find out the reason for the discrepancy between the DOPVEL period and the period obtained from the observations, simulations with an accurate period should help in determining if the discrepancy is due to instrumental problems. A more careful analysis of the accuracy in the calculations of the DOPVEL program needs to be made. The solution of this problem will make it possible to average several nights and obtain the long-term average pulse characteristics.

APPENDIX A
LIST OF PULSARS

Tables A-1 and A-2 contain the pulsar candidates to be observed using the University of Florida 26.3 MHz array and the 45 MHz array at the Maipu Radio Observatory

Table A-3 gives the references from which the data at the different frequencies were obtained.

Table A-1. Pulsar calibration [illegible] the Interplanetary Scintillation 26.3 MHz array.

Pulsar	Period (s)	DM ($pc\ cm^{-3}$)	Δt_D @ 8 KHz (ms)	Pulse Energy $\times 10^{-29}$ $Jm^{-2}Hz^{-1}$	Flux Density $\times 10^{-26}$ Jy	Pulse Width Half Intensity (ms)	Galactic Background Temp. (°K)	Zenith Angle at Transit (°)
0031-07	0.943	10	36.5	930 @ 61 MHz	1.0 @ 61 MHz	92 @ 102 MHz	32,550	37
0809+74	1.292	6	21.9	2,980 @ 61 MHz	2.3 @ 61 MHz	125 @ 61 MHz	66,855	44
0834+06	1.274	13	49.1	3,970 @ 61 MHz	3.1 @ 61 MHz	24 @ 61 MHz	24,660	24
1133+16	1.188	5	18.25	1,105 @ 53 MHz	0.75 @ 61 MHz	47 @ 61 MHz	27,620	14
1508+55	0.739	20	73	1,000 @ 61 MHz	1.35 @ 61 MHz	13 @ 102 MHz	20,713	25
1919+21	1.337	12	45.3	3,800 @ 61 MHz	2.8 @ 61 MHz	28 @ 102 MHz	78,908	9

Table A-2 List of pulsar candidates to be observed with Maipú [illegible] 45 MHz array.

Pulsar	Period (s)	DM ($pc\ cm^{-3}$)	Δt_D @ 10 KHz (ms)	Pulse Energy $\times 10^{-23}$ $Jm^{-2}Hz^{-1}$	Flux Density $\times 10^{-26}$ $Wm^{-2}Hz^{-1}$	Pulse Width Half Intensity (ms)	Galactic Background Temp (°K)	[illegible] Angle at Transit (°)
0031-07	0.94295	10.89	9.9	930 @ 61 MHz	1.0 @ 61 MHz	32 @ 102 MHz	~6,500	26
0628-28	1.24441	34.36	31.3	2,340 @ 61 MHz	1.5 @ 61 MHz	105 @ 61 MHz	~6,400	5
0826-34	1.84896	52	47.4	300 @ 408 MHz	N.A. (*)	775 @ 408 MHz	~6,400	0.5
0834+06	1.27376	12.85	11.7	3,970 @ 61 MHz	N.A. (*)	24 @ 61 MHz	<6,000	39
1749-28	0.56255	50.88	46.3	750 @ 80 MHz	>10 @ 34 MHz	~10 @ 408 MHz	~34,000	[illegible]
2045-16	1.96157	11.51	10.47	N.A. (*)	~1 @ 34 MHz	~83 @ 151 MHz	~8,500	[illegible]

(*) Information not available at that frequency.

Table A-3 List of references from which the data at the different frequencies was obtained.

Frequency MHz	References
34	Hacker (30)
53	Sieber (29)
61	Izvekova et al. (8)
80	Slee and Hill (9)
102	Izvekova et al. (7)
151	Lyne et al. (22)
408	Komesaroff et al. (10) and Manchester et al (38)

APPENDIX B
SAMPLING RATE, TIMING PULSE FREQUENCY AND DATA POINTS PER SECOND

For the configuration of the data reduction system used (Figure 2-2), the sampled values are sent to the Amdahl 470/V6 computer in real time. In that condition the rate of transmission of data into the Amdahl is the limiting factor for the sampling rate.

The absolute maximum transmission rate to the Amdahl 470/V6 is 1200 Baud (120 characters/second). The maximum useful rate is 60 characters/second; 40 characters/second is a more conservative (but reliable) rate. Since the A/D converter has 12 bits, which means 3 characters per data point, the transmission rate will be 40/3 = 13 data points per second.

The number of data points per second (DPS) obtained from the KIM I is given by the relationship (39):

$$DPS = \frac{1}{TPP \times NAVE \times TSAMP} \qquad (B-1)$$

where TPP = KIM I timing pulse period (ms)

NAVE = Number of sampled values averaged before sending to the terminal

TSAMP = Parameter for the KIM I program

The TPP for the KIM I must not be shorter than 4 ms (250 Hz); the value used in the digitizing process for the

pulsar was 8 ms (125 Hz). The number of sampled values averaged (NAVE) before sending through the terminal to the Amdahl is fixed at 8.

Table 8-1 gives the relationship between the TPP, TSAMP and the DPS (39)

Table 8-1. Values of DPS as a function of TPP and TSAMP.

TPP (ms)	FREQ (Hz)	TSAMP 01	02	03	04	05
4	250	31.25	15.625	10.4167	7.8125	6.250
8	125	15.075	7.8125	5.2083	3.906	3.125

Data Points Per Second (DPS)

In order to meet the transmission rate requirements of 13 data points per second using 8 ms for the TPP, a safe value of TSAMP = 02 must be used, that gives a value of 7.8125 DPS.

If the tapes are played back at the same speed that they are recorded, then the resolution would be also 7.815 DPS, which is a poor resolution. However, if the tapes are played back with a slow-down of 4:1 the time resolution will be increased by a factor of 4

Table 8-2 gives the number of DPS obtained in real time and in actual or original pulsar time (39).

[illegible] data points per second in real and original pulsar time.

	Samples per second			
[illegible]	1.1167	7.8125	6.250	5.2083
Original pulsar time	41.667	31.25	25.00	20.8332

Since NAVE is fixed at 8, that means that 8 sampled values are averaged together before producing one data point, in that way, the tape is being sampled 8 times faster than the data point rate. As an example, if a TPP = 8 ms and a TSAM = 02 are being used, 7.8125 DPS are obtained, but the tape is being sampled at the rate of 62.5 samples/second in real time, which in original pulsar time is 250 samples/second.

APPENDIX C
SCHEMATIC

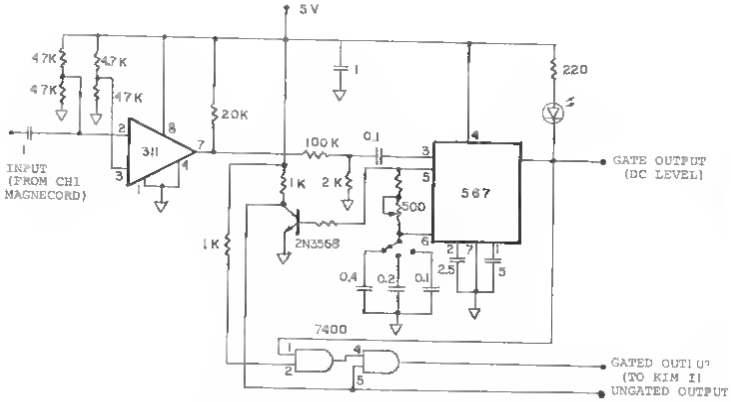

Figure C-1. Phase locked loop (PLL) schematic

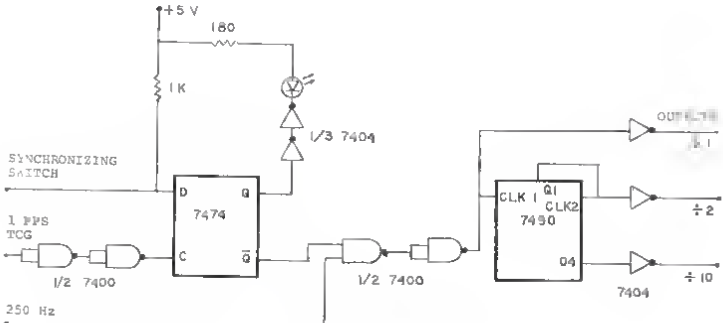

Figure C-2 Synchronizer and divider sch[illegible]

APPENDIX D
COMPUTER PROGRAMS

MCAPGM Program

MCAPGM1 Program

P2045 (or P1133) P[illegible]

```
[illegible]
... NUMBER OF ... [illegible]
```

APPENDIX E
26.3 MHz ARRAY CALIBRATION

In order to obtain the minimum detectable flux density and then estimate the peak flux density for pulsar PSR1133+16, several calibrations were performed with the array.

The standard noise source was provided by 2 Sylvania 5722 noise diodes; as a secondary noise source a Hewlett Packard amplifier was used. Several radio sources of known flux density and the galactic background temperatures were also used in the calibrations.

Figure E-1 is a block diagram of the 26.3 MHz array signal transmission and calibration system. Usually the calibration signals are introduced at point ① (Figure E-1). In order to improve the calibrations, the signal was later introduced at point ② (Figure E-1); by doing this, any uncertainties in the gain (or losses) of the 10 pre-amplifiers and the 2 N-S Butler matrices are avoided.

Two 1 input-to-6 outputs 50-ohm power splitters were used to split the calibration signal into the 10 preamplifier inputs. To properly match all the outputs, two power splitters output were loaded with 50-ohm resistors.

As a result of introducing the calibration signal at ① and then at ② , a net gain of ≈6 dB was determined for the 10 preamplifiers plus the 2 N-S Butler matrices, several

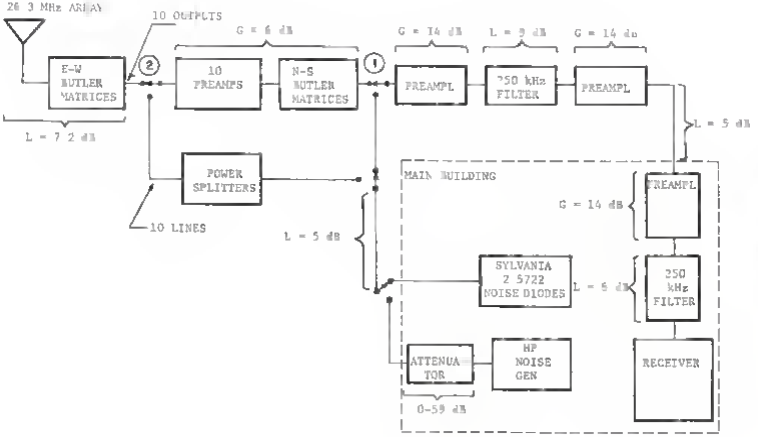

Figure E-1 Block diagram for the 26 3 MHz array calibration

other gains and losses were also determined for the preamplifiers, 250 KHz filters and aluminum coaxial lines; all the losses and gains determined are shown in Figure E-1

E.1 Losses Between the Dipoles and Point ②

The procedure to obtain the losses between the dipoles and point ②, which includes the 10 E-W Butler matrices, the hybrid rings, the matching networks and the parallel transmission lines, is not as straightforward as it is to obtain gain and losses for the rest of the system. An indirect method was therefore used in this thesis. First, the recorder deflection due to the galactic background was measured. Then a signal from the noise generator was introduced at point ② (using the indicated switch), and was adjusted to give the same recorder deflection as that from the galactic noise. From the ratio of the noise temperature of the introduced signal to that of the part of the sky from which the galactic signal was obtained, which is available in the literature, the losses can be obtained. A summary of the results is shown in Table E-1.

The noise temperature for the noise diodes has been calculated using the following relationship (17):

$$T = T_o + \frac{eIR}{2k} \qquad \text{(E-1)}$$

where T_o = ambient temperature (= 290°K)

e - electron charge (= 1.6×10^{-19} C)

I - diode's plate direct current

R = plate load resistance

k = Plank constant (= 1.38×10^{-23} J °K)

Table E-1. Summary of the readings and calibrations made in [illegible]

Right Ascension	Declination	Calibration at Point ① (dB)	Calibration at Point ② (dB)	Noise Temp. at Point ② (°K)	Corrected Noise Temp. at Point ② (°K)	Galactic Background Temp. (*) (°K)	[illegible]	[illegible]
$03^h\ 45^m$	7.6°	30.5	37	14,043	3,019	15,858	5.3	7.26
$14^h\ 50^m$	26.0°	29	34.7	23,881	5,063	25,000	4.93	6.94
$19^h\ 52^m$	26.0°	27	32.7	37,704	7,994	44,000	5.5	7.4
						Average Value	5.25	7.2

(*) Obtained from references (25, 40)

Subatituting in equation (E-1) the vaiuas for the constanta, using tha vaiue R = 50 ohm and axpressing I in milliamparas, the following relationahip can be daducad

$$T = 290 + 289.85\ I \qquad \text{(E-2)}$$

Equation E-2 givas tha tamparatura in °K and it is valid for R = 50 ohm.

Galactic background temparaturas for the first two points in tha sky have bean obtained from Turtle at al. (40) at 26.3 MHz. The value for the third point was obtainad from measurements made by Blythe (26) at 38 MHz and corractad to 26.3 MHz using the galactic background spactral indax given by Findlay (27) of n = 2.65, which is valid for tha ranga 20-400 MHz.

It is interesting to compara the lossaa obtained in Tabla E-1 with tha lossas obtained by aumming the astimatad dB attanuations along the path between the dipolas and point ②. Tha list of astimated or meaaurad losaas of tha individual components is givan in Tabla E-2 (41).

Tha average of tha maasurad lossas givan in Tabla E-1 is 7.2 dB which agraas well with tha lossas computed from Tabla E-2.

Table E-2. Losses between dipoles and point ② considering the partial losses.

	Minimum dB	Maximum dB
Full wave twin line	.30	.30
Hybrid ring	.45	.45
Phase cable	.80	1.10
Coaxial cable line	1.90	1.90
E-W Butler matrix	1.44	1.98
Line connecting E-W to N-S Butler Matrices	.5	1.10
Total	5.39	6.73

The corrected noise temperatures at point ②, given in Table E-1, is the noise temperature of the noise source corrected for the 5 dB losses in the aluminum coaxial line and the losses in the power splitter (factor 0.76); losses in the power splitter consider the losses due to the two 50-ohm resistors and the losses at 26.3 MHz of the power splitter itself.

E.2 Antenna Effective Area

By using the losses between the dipoles and point ② already obtained and calibrations done with radio source 3C433, the antenna effective area can be calculated; the method consists of obtaining the change in antenna temperatura

ΔT_a for a radio source of known flux density S. The relationship that gives the effective area is:

$$A_e = \frac{2k \Delta T_a}{S} \qquad (E-3)$$

ΔT_a is the change in antenna temperature referred to the dipoles, corrected for losses ϵ between point (2) and the dipoles. If $\Delta T'_a$ is the change in temperature measured at point (2), then the actual change in antenna temperature is:

$$\Delta T_a = \frac{\Delta T'_a}{\epsilon} \qquad (E-4)$$

where ϵ = transmission line efficiency, which in this case considers the losses between point (2) and the dipoles.

From the calibrations, the following values were obtained for 3C433.

$S = 267$ jy

$\Delta T'_a = 295°K$

$T_a = 25{,}000°K$

$\epsilon = 0.19$

Using equations E-3 and E-4, the following value is obtained:

$$A_e = 16{,}050 \text{ m}^2$$

This value needs to be corrected by a factor $p_1 = 0.69$, given in the Array program (11), which considers the fact that the source is off the center of the beam. The corrected effective area of the antenna is then:

$$A_e = 23{,}260 \text{ m}^2$$

The value of the effective area can be also expressed in terms of the change in antenna temperature in °K, divided by the flux density in Jy (°K/Jy), this quantity is usually denoted as A_e^* (12)

$$A_e^* = \frac{\Delta T_a \times p_1}{S} \qquad \text{(E-5)}$$

Substituting in E-5 the values

$\Delta T_a = \Delta T_a'/\epsilon = 1553°K$

$S = 267$ Jy

$p_1 = 0.69$

the following value for A_e^* is obtained

$A_e^* = 8.3$ °K/Jy

LIST OF REFERENCES

1. A. Hewish, S. J. Bell, J. D. H. Pilkington, P. F. Scott, R. A. Collins, "Observations of a Rapidly Pulsating Radio Source," Nature, 217, 709 (1968).

2. Yu. M. Bruck, J. G. Davies, A. D. Kuz'min, A. G. Lyne, V. M. Molofeev, B. Rowson, B. Yu. Ustimenko and Yu. P. Shitov, "Radio-emission Spectra of Five Pulsars in the 17-1420 MHz Range," Soviet Astronomy, 22, 583 (1979).

3. F. N. Bash, F. A. Bozyan and G. W. Torrence, "Observations of CP1919 and NP0532 at 38 MHz," Astrophysical Letters, 7, 39 (1970).

4. Yu. M. Bruck and B. Yu. Ustimenko, "Decametric Pulse Radio Emission from PSRD809, PSR1133, and PSR1919," Nature Physical Science, 242, 58 (1973).

5. Yu. M. Bruck and B. Yu. Ustimenko, "Decametric Radio Emission from Four Pulsars," Nature, 260, 766 (1976).

6. H. D. Craft Jr. and J. M. Comella, "Frequency Dependent Pulse Width for CP1133," Nature, 220, 676 (1968).

7. V. A. Izvekova, A. D. Kuz'min, V. M. Molofeev and Yu. P. Shitov, "Energy Spectra and Pulse Shapes of Pulsars at Metre Wavelengths," Australian Journal of Physics, 32, 25 (1979).

8. V. A. Izvekova, A. D. Kuz'min, V. M. Molofeev and Yu. P. Shitov, "Radio Flux Density and Pulse Profile of Pulsars at 102.5 and 61 MHz," Soviet Astronomy, 23, 179 (1979).

9. O. B. Slee and E. R. Hill, "Pulsar Energy Fluxes at 80 MHz," Australian Journal of Physics, 24, 441 (1971).

10. M. M. Komesaroff, D. Morris and D. J. Cooke, "Linear Polarization and Pulse Shape Measurements on Nine Pulsars," Astrophysical Letters, 5, 37 (1970).

11. M. D. Desch, "26.3 MHz Array Reference Manual," unpublished.

12. M. D. Desch, Ground Based and Spacecraft Studies of Jupiter at Decameter and Hectometer Wavelengths (Ph.D. Dissertation, University of Florida, 1976).

13. M. D. Desch, T. D. Carr and J. Levy, "Observations of Jupiter at 26.3 MHz Using a Large Array," Icarus, 25, 12 (1975).

14. P. Reyes, Radiotelescopio en 45 MHz para Fuentes Extragalacticas, Memoria para optar al titulo de Ingeniero Civil Electricista (Thesis, University of Chile, 1977).

15. J. May, P. Reyes and J. Aparici, "A 45 MHz Radiotelescope for Galactic and Extragalactic Research," First Latin-American Regional Astronomy Meeting, Santiago, Chile (1978).

16. M. R. Viner and W. C. Erickson, "26.3 MHz Radio Source Survey. II. Radio Sources Positions and Fluxes," The Astronomical Journal, 80, 931 (1975).

17. J. D. Kraus, Radio Astronomy (Mac Graw Hill Inc., New York, 1966).

18. G. R. Huguenin, R. N. Manchester and J. H. Taylor, "Properties of Pulsars," The Astrophysical Journal, 169, 97 (1971).

19. F. D. Drake and H. D. Craft, "Pulse Structure of Four Pulsars," Science, 160, 758 (1968).

20. A. D. Kuz'min, V. M. Molofeev, Yu P. Shitov, J. G. Davies, A. G. Lyne and A. Rowson, "Spectra of Nine Pulsars at 61-1420 MHz," Monthly Notices of the Royal Astronomical Society, 185, 441 (1978).

21. R. D. Ekers, A. T. Moffet, 'Further Observations of Pulsating Radio Sources at 13 cm," Nature, 220, 756 (1968).

22. A. G. Lyne, F. G. Smith and D. A. Graham, "Characteristics of the Radio Pulses from the Pulsars," Monthly Notices of the Royal Astronomical Society, 153, 337 (1971).

23. J. May and J. Aparici, Personal Communication (1980).

24. B. Y. Mills, B. Slee and E. R. Hill, "A Catalogue of Radio Sources Between Declinations +10° and -20°," Australian Journal of Physics, 11, 300 (1958)

25. O. B. Slee, "Culgoora-3 List of Radio Source Measurements," Australian Journal of Physics, Astrophysical Supplements, Number 43, (Nov., 1977).

26. J. H. Blythe, "Results of a Survey of Galactic Radiation at 38 MHz," Monthly Notices of the Royal Astronomical Society, 117, 652 (1957)

27. J. W. Findlay, "Absolute Intensity Calibrations in Radio Astronomy, Annual Review of Astronomy and Astrophysics, 4, (1966)

28. A. J. Turtle, A. E. Vaughan, "Discovery of Two Southern Pulsars," Nature, 219, 689 (1968)

29. W. Sieber, "Pulsar Spectra. A Summary," Astronomy and Astrophysics, 28, 237 (1973).

30. D. C. Backer, Personal Communication to S. T. Gottesman (1975)

31. R. N. Manchester and J. H. Taylor, Pulsars, (W. H. Freeman and Co, San Francisco, 1977).

32. R. N. Manchester, J. B. Taylor, G. R. Huguenin, "Observations of Pulsars Radio Emission II. Polarization of Individual Pulses," Astrophysical Journal, 196, 83 (1975)

33. G. R. Huguenin, R. N. Manchester and J. H. Taylor, "Properties of Pulsars," Astrophysical Journal, 169, 97 (1971).

34. J. D. H. Pilkington, A. Hewish, S. J. Bell and T. W. Cole, "Observations of Some Further Pulsed Radio Sources," Nature, 218, 126 (1968)

35. Yu. I. Alekseev and S. A. Suleimanova, "Polarimetry of Pulsars at 3.5 m Wavelength," Soviet Astronomy, 21, No. 2, 180 (1977).

36. Yu. P. Shitov, "Fine Structure of Pulsar Radio Spectra," Soviet Astronomy, 16, 383 (1972).

37. R. N. Manchester, "Pulsar Rotation and Dispersion Measures and the Galactic Magnetic Field," The Astrophysical Journal, 172, 43 (1972)

38 R N Manchester, A. G. Lyne, J H. Taylor, J. M. Durdin, M I. Large and A G Little, "The Second Molonglo Pulsar Survey - Discovery of 155 Pulsars, Monthly Notices of the Royal Astronomical Society, 185, 409 (1978).

39. J. P. Oliver, Personal communication (1978).

40. A. J. Turtle, J. F. Pugh, S Kenderdine and I. I. K. Pauliny-Toth, "The Spectrum of the Galactic Radio Emission,' Monthly Notices of the Royal Astronomical Society, 124, 297 (1962).

41 J Levy, Personal communication (1980).

BIOGRAPHICAL SKETCH

Patricio Reyes was born in Santiago, Chile, on December 8, 1941. After finishing high school and with a strong desire to study electrical engineering (in which he was encouraged by his parents, sisters and brother), he entered the School of Engineering of the University of Chile. It was there where he became interested in astronomy while taking a course with Professor Claudio Angulta. His interest grew when he was allowed to use the old Heide refractor at Cerro Calán. He started his amateur astronomical activities by building his own small Newtonian reflector and spending hours and hours watching the interesting southern sky (in which he was enthusiastically supported by his two sisters Lucia and Guadalupe and his brother Juan).

His professional interest turned to radio astronomy when in 1974 Jorge May asked him to work on the 45 MHz array in Maipú as a thesis project.

In 1975 he married Maria Angelica, and they now have two daughters: Carolina and Daniela (who just joined the family).

In 1977 he obtained a degree in electrical engineering from the University of Chile, and in September of the same year

he came to the University of Florida to continue his studies in astronomy. While studying at the University of Florida he has been teaching elementary physics laboratories, elementary astronomy laboratories and digital electronics laboratories.

His other interests are mountain climbing, Andean music and photography.

I certify that I have read this study and that in my opinion it conforms to acceptable standards of scholarly presentation and is fully adequate, in scope and quality, as a thesis for the degree of Master of Science

Thomas D. Carr

Thomas D Carr, Chairman
Professor of Astronomy
and Physics

I certify that I have read this study and that in my opinion it conforms to acceptable standards of scholarly presentation and is fully adequate, in scope and quality, as a thesis for the degree of Master of Science

Alex G. Smith

Alex G Smith
Professor of Astronomy
and Physics

I certify that I have read this study and that in my opinion it conforms to acceptable standards of scholarly presentation and is fully adequate, in scope and quality, as a thesis for the degree of Master of Science.

John P. Oliver
Associate Professor of Astronomy

This thesis was submitted to the Graduate Faculty of the Department of Astronomy in the College of Liberal Arts and Sciences and to the Graduate Council, and was accepted as a partial fulfillment of the requirements for the degree of Master of Science.

December, 1980

Dean, Graduate School